© 2020. Published by The Company of Biologists Ltd | Development (2020) 147, dev185710. doi:10.1242/dev.185710

STEM CELLS AND REGENERATION

RESEARCH ARTICLE

A coherent feed-forward loop drives vascular regeneration in damaged aerial organs of plants growing in a normal developmental context

Dhanya Radhakrishnan[1,*], Anju Pallipurath Shanmukhan[1,*], Abdul Kareem[1,*], Mohammed Aiyaz[1,*], Vijina Varapparambathu[1], Ashna Toms[1], Merijn Kerstens[2], Devisree Valsakumar[1], Amit N. Landge[1], Anil Shaji[1], Mathew K. Mathew[1,3], Megan G. Sawchuk[4], Enrico Scarpella[4], Beth A. Krizek[5], Idan Efroni[6], Ari Pekka Mähönen[7,8], Viola Willemsen[2], Ben Scheres[2] and Kalika Prasad[1,‡]

ABSTRACT

Aerial organs of plants, being highly prone to local injuries, require tissue restoration to ensure their survival. However, knowledge of the underlying mechanism is sparse. In this study, we mimicked natural injuries in growing leaves and stems to study the reunion between mechanically disconnected tissues. We show that *PLETHORA* (*PLT*) and *AINTEGUMENTA* (*ANT*) genes, which encode stem cell-promoting factors, are activated and contribute to vascular regeneration in response to these injuries. PLT proteins bind to and activate the *CUC2* promoter. PLT proteins and CUC2 regulate the transcription of the local auxin biosynthesis gene *YUC4* in a coherent feed-forward loop, and this process is necessary to drive vascular regeneration. In the absence of this PLT-mediated regeneration response, leaf ground tissue cells can neither acquire the early vascular identity marker ATHB8, nor properly polarise auxin transporters to specify new venation paths. The PLT-CUC2 module is required for vascular regeneration, but is dispensable for midvein formation in leaves. We reveal the mechanisms of vascular regeneration in plants and distinguish between the wound-repair ability of the tissue and its formation during normal development.

KEY WORDS: Vascular regeneration, PLT, CUC2, Wound repair, Auxin, PIN1, *Arabidopsis*

INTRODUCTION

Plants are prone to numerous injuries in their lifespan, owing to their sessile lifestyle. They are subjected to injuries caused by biotic factors such as pathogen attack and herbivory. Abiotic factors such as damaging weather conditions can also cause tissue damage. Unhealed wounds can compromise plant fitness and survival, and tissue-healing mechanisms have evolved to counteract the damage. Following wounding, regenerative responses may be restricted to local healing in the form of cell proliferation or may entail complete regeneration of damaged tissue or organ (Ikeuchi et al., 2016; Galliot et al., 2017). The capacity of plants to regenerate the complete body plan *in vitro* from excised tissue is a powerful demonstration of the versatility of plant regeneration processes and forms the basis for many horticultural applications (Kareem et al., 2015; Ikeuchi et al., 2016; Radhakrishnan et al., 2018).

In stem, cellular, molecular and hormonal interactions at wound sites coordinate wound healing and restore vasculature (Flaishman et al., 2003; Asahina et al., 2011; Pitaksaringkarn et al., 2014; Melnyk et al., 2015; Mazur et al., 2016). Auxin is important for vascular tissue regeneration in multiple plant species (Sachs, 1968, 1969, 1981, 1991). The canalization models that underlie this regeneration process rely on the potential of auxin to induce correctly polarised auxin transporters together with activation of vascular cell fate determinants (Wenzel et al., 2007; Donner et al., 2009; Ohashi-Ito et al., 2013). In the growing tips of shoots and roots, damaged meristematic cells are replaced using positional cues from neighbouring cells (van den Berg et al., 1995; Reinhardt et al., 2003).

In roots, regeneration involves reactivation of embryo-specific genes, proper reallocation of root cell-fate determinants and integration of auxin, cytokinin and jasmonate signals (Xu et al., 2006; Efroni et al., 2016; Marhava et al., 2019; Zhou et al., 2019).

Laser ablation and root tip resection studies have shown that stem cell activation is a vital step for regeneration of lost cells and entire organs (van den Berg et al., 1995; Xu et al., 2006; Marhava et al., 2019; Zhou et al., 2019). The stem cell regulators PLETHORA1 (PLT1) and PLT2 are essential for the re-establishment of quiescent centre (QC) cells upon laser ablation and for the regeneration of primary and lateral root tips following resection (Xu et al., 2006; Durgaprasad et al., 2019). *PLT1* and *PLT2* are induced by PLT3, PLT5 and PLT7 activity to regulate stem cell activation during lateral root development (Du and Scheres, 2017). In the shoot, members of the PLT family along with the transcription factor AINTEGUMENTA (ANT) regulate the development and phyllotaxis of aerial organs (Prasad et al., 2011; Krizek, 2015). PLT factors also regulate hormone-mediated *de novo* shoot regeneration (Kareem et al., 2015).

Although several studies have addressed specific regeneration processes in specific plant parts or in excised organs and have implicated certain factors regulating these processes, our knowledge of the underlying molecular mechanisms of wound repair in aerial organs is limited (Ikeuchi et al., 2018). It is largely unknown how

[1]School of Biology, Indian Institute of Science Education and Research, Thiruvananthapuram 695551, India. [2]Plant Developmental Biology, Wageningen University Research, Wageningen 6708 PB, The Netherlands. [3]National Centre for Biological Sciences, Tata Institute of Fundamental Research, 15, Bengaluru, 560065, India. [4]Department of Biological Sciences, University of Alberta, Edmonton, Alberta T6G 2E9, Canada. [5]Department of Biological Sciences, University of South Carolina, Columbia, SC 29208, USA. [6]The Robert H. Smith Institute of Plant Sciences and Genetics in Agriculture, The Hebrew University, Rehovot 76100, Israel. [7]Institute of Biotechnology HiLIFE, University of Helsinki, 00014 Helsinki, Finland. [8]Organismal and Evolutionary Biology Research Programme, Faculty of Biological and Environmental Sciences, Viikki Plant Science Centre, University of Helsinki, 00014 Helsinki, Finland.
*These authors contributed equally to this work

‡Author for correspondence (kalika@iisertvm.ac.in)

B.A.K., 0000-0001-5821-0180; I.E., 0000-0002-0219-8685; K.P., 0000-0001-8666-856X

Received 15 October 2019; Accepted 17 February 2020

Development (2020) 147, dev185710. doi:10.1242/dev.185710

wound repair in leaf tissue relates to the normal developmental programme. Here, we investigate vascular reprogramming after leaf damage from the viewpoint that tissue reprogramming may require stem cell factors identified in other regeneration contexts. We reveal an essential role of members of the *PLETHORA* (*PLT*)/*AINTEGUMENTA* (*ANT*) gene family in activating regeneration responses. *PLT* genes act through *CUP-SHAPED COTYLEDON2* (*CUC2*) to repair wounds and regenerate vascular tissue in damaged aerial organs. Furthermore, we show that the *PLT-CUC2* module acts through local auxin biosynthesis, and is required for proper repolarisation of PIN1 auxin efflux facilitators and reprogramming of vascular identity in aerial organs. The *PLT-CUC2* module is strictly required for regeneration of leaf vasculature, but is not essential for the normal development of closed vein loops in the absence of perturbations.

RESULTS

PLT3, *PLT5* and *PLT7* genes respond dynamically to mechanical injuries

PLT3, *PLT5* and *PLT7* collectively regulate tissue culture-mediated *in vitro* shoot regeneration and will from here on be referred to as *PLT3,5,7*. *PLT3,5,7*-regulated root stem cell regulators establish pluripotency in calluses and *PLT3,5,7*-regulated shoot-promoting factors act in response to external hormonal cues to induce regeneration of the complete plant body (Kareem et al., 2015).

Interestingly, *PLT3,5,7* genes are expressed in the shoot during development and positioning of aerial organs (Prasad et al., 2011; Krizek, 2015). To assess whether PLT3,5,7 function is required for repairing damaged inflorescence and leaf tissue without external hormonal cues, we determined whether expression of these genes is induced as a natural response to injuries that growing plants are likely to encounter, such as local abrasions in the stem, partial stem incisions and midvein injuries in the leaf blade. These injuries were made without detaching any organ from growing *Arabidopsis* plants. After local abrasion that damaged the epidermal and sub-epidermal layers, including vascular tissue, in inflorescence stem (Fig. 1A,A′, Fig. S1A-D), *PLT7::PLT7-vYFP* was induced 12 h post-injury, prior to any apparent regeneration response (Fig. 1B,B′). The expression peaked at 36 h (Fig. 1C,C′, Fig. S1F,F′). In response to partial incision of the inflorescence stem (Fig. 1D,D′), *PLT7::PLT7-vYFP* expression was upregulated at both ends of the incised stem, with relatively higher expression in the upper end after 6 h (Fig. 1E,E′). The high level of expression continued for 12 h (Fig. 1F,F′). At 12 h, upregulated expression expanded beyond the partial slit, and at 24 h it became confined to a narrower domain in the vicinity of the incision (Fig. 1F-G′). Transcript levels of *PLT7* were consistent with the fusion protein expression data and remained upregulated at 24 h (Fig. S1E). Similarly, when the midvein of a growing leaf blade was wounded, cells in the vicinity displayed pronounced upregulation of *PLT7::PLT7-vYFP* 12 h post-injury (Fig. 1H,I). In response to injury, *PLT3::PLT3-vYFP* and *PLT5::PLT5-vYFP* also showed upregulation of expression in the vicinity of the wound albeit with some differences in the timing of their activation and in spatial distribution (Fig. 1J,K, Figs S1G-P′, S2 and S3). In response to leaf incision, although both PLT3 and PLT7 were expressed in close proximity to the wound, PLT5 was expressed predominantly in the vascular tissue near the damage (Fig. 1H-K, Fig. S3A,B).

The root stem cell regulators *PLT1*, *PLT2* and *WOX5*, which are activated by PLT3,5,7 during tissue culture-mediated *in vitro* shoot regeneration (Kareem et al., 2015), were not expressed in growing leaves and stems in response to injuries (Fig. S4).

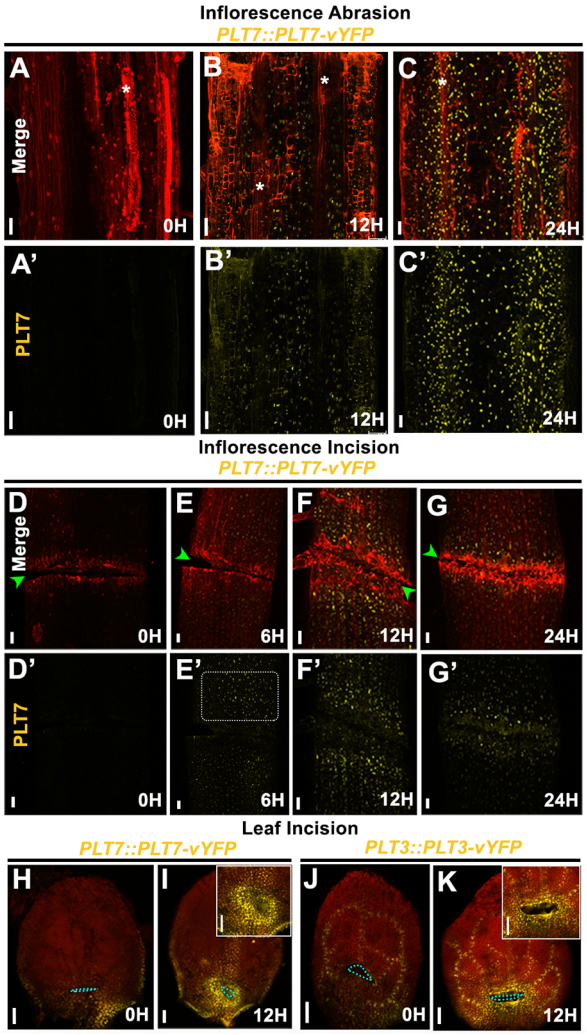

Fig. 1. *PLT3*, *PLT5* and *PLT7* genes are locally induced after mechanical injury. (A-G′) *PLT7::PLT7-vYFP* expression (yellow) after abrasion (A-C′) and partial incision (green arrowheads) (D-G′) in growing inflorescence stems. White asterisks indicate vascular tissues exposed by damage to epidermal and sub-epidermal layers following local abrasion. E′ white dotted area highlights upregulation of *PLT7* expression at the upper end of the cut. A′-C′ and D′-G′ are maximum intensity projections of *z*-stacks in the YFP channel corresponding to the regions shown in A-C and D-G, respectively. (H-K) Upregulation of *PLT7::PLT7-vYFP* (H,I) and *PLT3::PLT3-vYFP* (J,K) (yellow) near wound site (insets) following leaf incision (blue dotted area indicates the incision site). The panels represent different samples at each time point. Red signal is propidium iodide staining in A-G and chlorophyll autofluorescence in H-K. Brightness of the YFP signal was increased for visibility in B, B′ and E′. H, hours after injury. Scale bars: 50 µm.

PLT3,5,7 are required to activate innate regenerative responses to injuries in aerial organs

Aerial organs of growing plants are subject to substantial wear and tear and *PLT3,5,7* expression is rapidly activated in response to injuries (Fig. 1, Figs S1-S3). We therefore asked whether *PLT3,5,7* genes are required for wound repair and tissue regeneration in stems and leaves growing in the normal developmental context of *Arabidopsis*.

Wound repair and vascular regeneration in inflorescence stem

We mimicked physical abrasion by damaging the epidermis, sub-epidermal layers and vascular tissue locally (see Materials and Methods for details; Fig. 2A,A′) in a growing inflorescence stem of wild-type as well as *plt3;plt5-2;plt7* mutant plants. In the wild type,

Development (2020) 147, dev185710. doi:10.1242/dev.185710

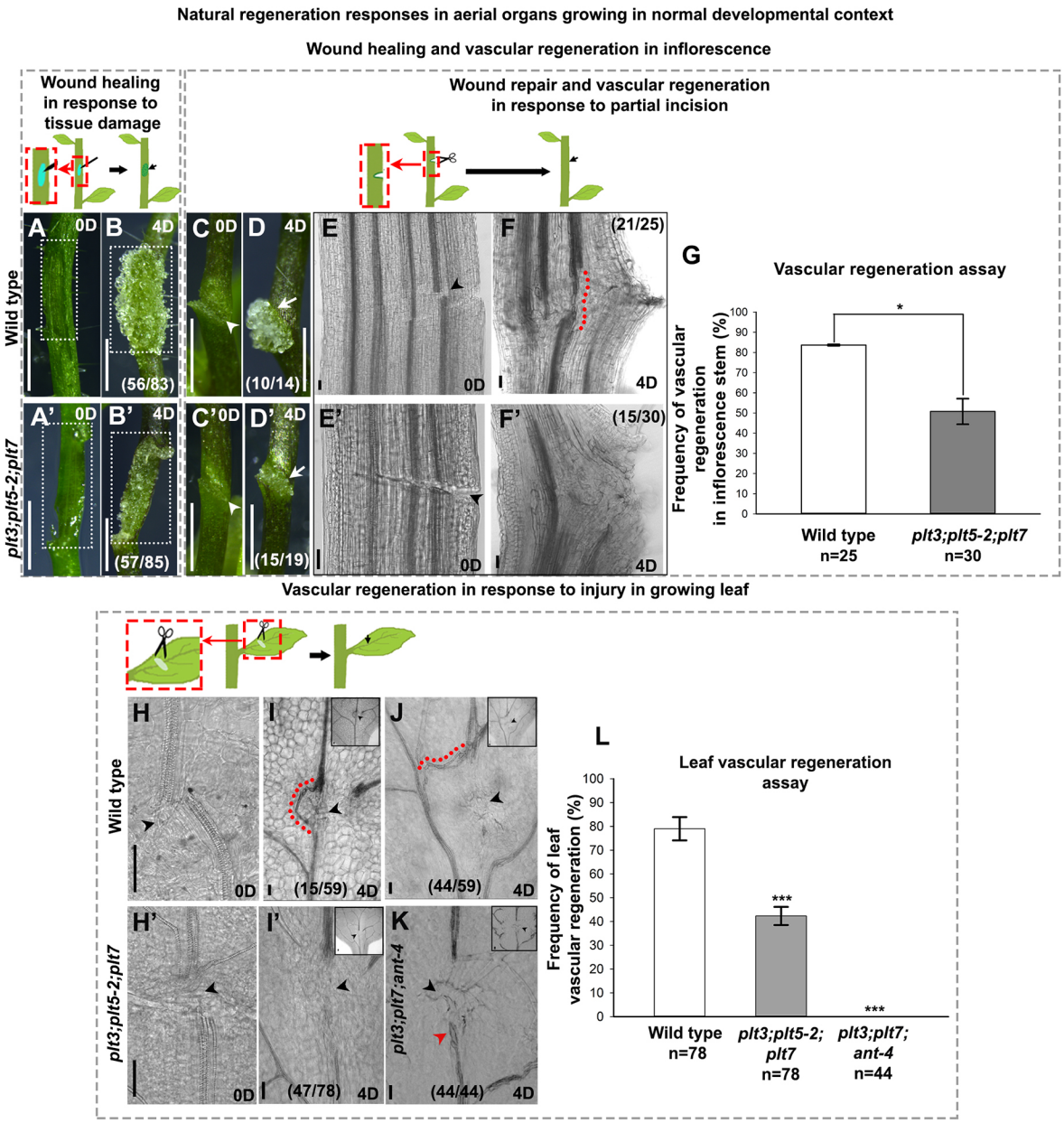

Fig. 2. *PLT* genes activate innate regenerative responses to injuries in aerial organs growing in the normal developmental context. (A-F′) Schematics above A and B represent inflorescence stem abrasion (red rectangle; cyan indicates wounded region) and wound healing response (arrow). Wound healing and vascular regeneration in inflorescence stems. (A,A′) Abrasion (dotted rectangles) in inflorescence stems of wild type (A) and *plt3;plt5-2;plt7* (A′). (B,B′) Reduced wound healing response (dotted rectangles indicate area of cell proliferation) in *plt3;plt5-2;plt7* (B′) compared with wild type (B). (C,C′) Partial incision (white arrowheads) in inflorescence stems of wild type (C) and *plt3;plt5-2;plt7* (C′). (D,D′) Compromised callus formation (white arrows) in inflorescence stems of *plt3;plt5-2;plt7* (D′) compared with wild type (D). (E,E′) Disruption of vascular tissue (black arrowheads) by partial incision in inflorescence stems of wild type (E) and *plt3;plt5-2;plt7* (E′). (F,F′) Vascular strands regenerate in wild-type inflorescence stems (F) but fail to regenerate in ∼49% of *plt3;plt5-2;plt7* stems (F′). Schematics above E and F indicate partial incision on inflorescence stem (red rectangle) and wound healing response. Black arrow indicates site of wound healing. (G) Frequency of vascular regeneration in response to partial incision in the inflorescence stems of wild type and *plt3;plt5-2;plt7* (**P*=0.033; Pearson's χ^2 test). Schematics above H and I indicate incision in the midvein of the growing leaf (red rectangle). The wound is repaired by vascular regeneration and local cell proliferation. (H-K) Vascular strand regeneration in the growing leaf. (H,H′) Incision (black arrowheads) in the midvein of wild-type (H) and *plt3;plt5-2;plt7* (H′) growing leaves. (I) Vascular strands regenerate in the wild-type leaf, bypassing the wounded area and connecting the cut ends of the midvein. (J) A new vascular strand connects the upper cut end of the midvein to the lateral vein. Red dotted line in I and J indicate the regenerated vascular strand. (I′,K) Vascular strands failed to regenerate in 60% of *plt3;plt5-2;plt7* leaves (I′). *plt3;plt7;ant-4* (K) mutant leaves completely failed to regenerate in response to midvein injury. Red arrowhead indicates proliferating cells at the lower cut end of the midvein. Insets show lower magnification images of the site of injury. Black arrowheads indicate the incision site. (L) Frequency of leaf vascular regeneration in wild type, *plt3;plt5-2;plt7* mutants (****P*=1.211×10^{-15}; Pearson's χ^2 test) and *plt3;plt7;ant-4* mutants (****P*=7.707×10^{-13}; Pearson's χ^2 test). Error bars represent s.e.m. In image panels, sample numbers are shown in parentheses. Scale bars: 1 mm (A-D′); 50 µm (E-F′,H-K). D, days after injury.

we noticed a healing response in the form of a visible mass of proliferating cells (callus-like growth) throughout the wound at 2 days after abrasion (daa), which became more prominent at 4 daa (Fig. 2B, Fig. S5A,B). Later, callus-like growth completely covered and sealed the wound. The inflorescence stem regained its growth following the repair process. In contrast to wild type, the healing

Development (2020) 147, dev185710. doi:10.1242/dev.185710

response was severely reduced in injured *plt3;plt5-2;plt7* inflorescence stems and the wound-sealing process was not completed in the triple mutant inflorescence stem (Fig. 2A′,B′, Fig. S5A′,B′). Importantly, the inflorescence stem development of uninjured mutant was comparable to that of wild type (Fig. S5I,J).

Next, we made a partial slit in the inflorescence stem of wild-type and *plt3;plt5-2;plt7* mutant plants disrupting both vascular connections and ground tissue (Fig. 2C,C′,E,E′). Twenty-four hours after the incision, the wounded parts adhered in the wild-type inflorescence stem (Fig. S5C,D). Subsequently, cell proliferation was observed as indicated by visibly swollen tissues at cut ends followed by regeneration of vascular tissues at 4 days after cut (dac) (Fig. 2D,F). Subsequent restoration of growth and physiological functions were demonstrated by the development of new flowers and siliques (Fig. S5E). In contrast to wild type, in which the wound was healed on the fourth day, the *plt3;plt5-2;plt7* triple mutant displayed severely reduced callus-like growth at the wound site and ∼49% inflorescence stems failed to regenerate vascular tissue (Fig. 2C′-F′, G, Fig. S5C′). Our data demonstrate the role of *PLT3,5,7* in activating a healing response in the form of callus-like growth and vascular regeneration to restore damaged tissue in a growing inflorescence stem.

Vascular regeneration in a growing leaf

Restoration of vasculature is a long-known feature of stem regeneration, and we investigated whether this response also occurred in leaves. We made a local injury in the midvein of a growing young wild-type leaf of a 5 days post-germination (dpg) plant (see Materials and Methods). To keep the developmental stage uniform, we injured the first pair of young leaves, which displayed midvein formation but not fully developed lateral veins at the time of injury (Fig. 2H,H′, Fig. S6A,A′). The injuries either (1) damaged the midvein without making an opening or (2) completely disconnected the midvein leaving a gap between the vascular strands. In both the cases, cells in the vicinity of the midvein experienced mechanical perturbations due to the pressure applied by the needle. Four days post-injury (dpi), wild-type leaves repaired both types of injuries. In case (1), where the break was incomplete, the injured midvein was repaired and new vascular cells regenerated to restore the physiological connection (Fig. S6E). In case (2), where there was a complete disconnection, we observed regeneration of the vascular strand either connecting together the cut ends of the midvein or connecting the cut end of the midvein to a lateral vein (Fig. 2I,J, Fig. S6F,G). Strikingly, after local injury in the midvein of young wild-type leaf blades, ∼80% of the samples regenerated vascular tissue in response to incision (Fig. 2L). The regenerating vascular cells often bypassed the damaged area and reunited with the lower half of the midvein making a D-shaped loop around the wound site similar to Sachs' observation of vascular regeneration around the wound site in the epicotyl stem of pea plants (Sachs, 1981) (Fig. 2I). Alternatively, they formed a new connection to the nearest lateral vein (Fig. 2J). The non-regenerating lower vascular strand degenerated after residual proliferation at the cut end (Figs S5L and S6B). We followed vascular regeneration from the time of injury to distinguish between the vascular strand reuniting the midvein regenerating from the cut end and the recruitment of a pre-existing lateral vein developed during leaf growth (Fig. S6A-D′). When the injury left a hole in the leaf blade exceeding 400 µm between the cut ends of the midvein, we rarely observed any vascular regeneration (Figs S6H,I and S7A). Such injuries left behind only a disorganised mass of cells (Fig. S6H). We therefore restricted our subsequent analysis to leaf blade injuries that completely disconnected the midvein leaving a gap well under 400 µm between the cut ends.

In contrast to wild-type leaves, in which ∼80% of the injured leaves regenerated vascular strands, only ∼40% of injured *plt3;plt5-2;plt7* leaves could regenerate and the rest completely failed to regenerate vascular strands (Fig. 2H′,I′,L). In non-regenerating mutant leaves, lateral veins failed to connect to the midvein near the wound site (Fig. 2I′), but a disorganised mass of proliferating cells at the wound site was observed, mostly at the cut ends of upper vascular strands and on the epidermis (Fig. S7B-D). Many such leaves displayed poor growth and failed to develop properly (Fig. S7E). It is important to note that uninjured *plt3;plt5-2;plt7* mutant plants did not display any defects in the formation of closed vein loops (consisting of midvein and secondary veins) compared with wild type but were severely impaired in vascular regeneration (Fig. 2L, Fig. S7F-I). With respect to leaf morphology, we did not observe any defects in the first pair of leaves (Fig. S5F,G). Among double mutant combinations, 70% of *plt3;plt5-2* and *plt5-2;plt7* double mutants regenerated vascular strands in response to injury, and only ∼64% of *plt3;plt7* double mutant leaves regenerated vascular tissue (Fig. S8A).

The closely related *AINTEGUMENTA* (*ANT*) gene marks stem cells of root vascular cambium and acts redundantly with *PLT3* and *PLT7* during plant development (Krizek, 2015; Smetana et al., 2019). *ANT* is strongly expressed in the vascular tissue of young leaves (Fig. S8B). We therefore examined vascular regeneration in *plt3;plt7;ant-4* triple mutant plants in response to midvein injury. Strikingly, none of the tested *plt3;plt7;ant-4* seedlings regenerated vascular tissues, demonstrating an essential role of *ANT* with *PLT3* and *PLT7* in vascular regeneration (Fig. 2K,L, Fig. S8C). Taken together, our data reveal a previously unrecognised role of *PLT3,5,7* and *ANT* in repairing damaged tissues during plant growth.

Because of the severity of shoot phenotypes in *plt3;plt7;ant-4* (which produces only leaves but no stem) we chose the *plt3;plt5-2;plt7* mutant, which develops normal leaves as well as an inflorescence stem comparable to wild type, to probe the mechanism of vascular regeneration using further assays (Prasad et al., 2011; Krizek, 2015).

PLT5 and *PLT7* are sufficient for promoting vascular regeneration and wound repair

Tissue/organ regeneration is closely linked to cellular reprogramming. We next asked whether *PLT* genes are sufficient to activate cellular reprogramming leading to enhancement of wound repair. Strikingly, inducible overexpression of PLT5 (*35S::PLT5-GR*) or PLT7 (*35S::PLT7-GR*) promoted multiple strand formation from the regenerating midvein in response to injury (Fig. 3A,A′,C,C′, Fig. S8D). Similarly, inducible overexpression of PLT5 or PLT7 enhanced wound repair at the cut ends of the detached organ and in response to inflorescence abrasion (Fig. 3B,B′,D,D′, Fig. S8E-F′). Consistent with the ability of PLT proteins to promote cell division upon wounding, transcripts of *CYCLIN* genes increased in growing seedlings upon inducible overexpression of PLT5 (*35S::PLT5-GR*) (Fig. S8G). These results suggest that PLT proteins are sufficient to promote wound repair and multiple vascular strand regeneration in response to injury.

We addressed whether PLT-like proteins from other plant species can trigger regeneration in *Arabidopsis*. Rice is a morphologically diversified monocot plant, whereas *Arabidopsis* is a dicot. Expression of the rice *PLT*-like gene *OsPLT2* under the *Arabidopsis PLT5* promoter in a *plt3;plt5-2;plt7* mutant (*plt3;plt5-2;plt7;AtPLT5::OsPLT2-vYFP*) healed a damaged *Arabidopsis plt* mutant inflorescence stem by inducing cell proliferation as evident from upregulated expression of cell cycle progression markers (Fig. 3E-G, Fig. S8H,I). Furthermore, *OsPLT2-vYFP* rescued leaf vascular regeneration defects in *plt3;plt5-2;plt7* suggesting that it is a functional homologue of *Arabidopsis PLT* genes (Fig. 3H-J).

Development (2020) 147, dev185710. doi:10.1242/dev.185710

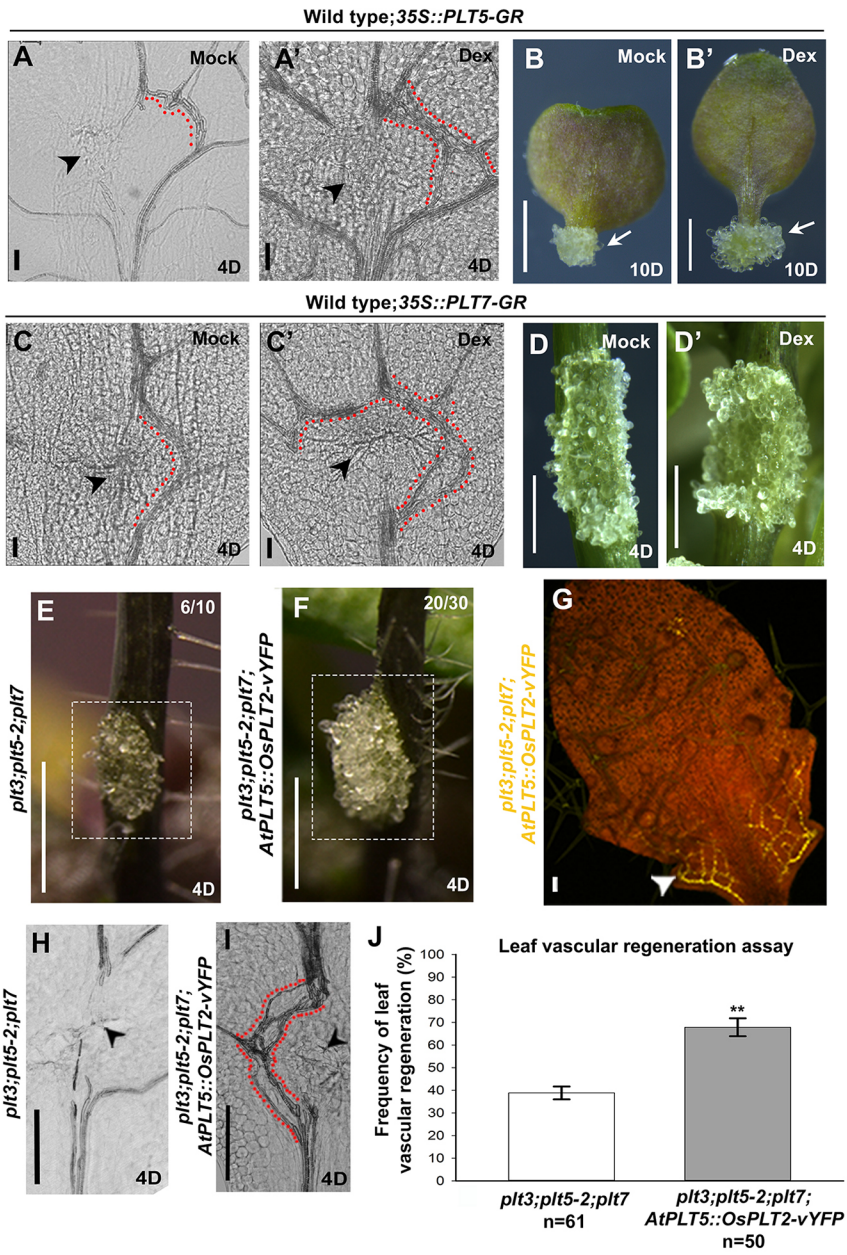

Fig. 3. *PLT* genes are sufficient for enhancing vascular regeneration and wound repair. (A-B′) Overexpression of *35S::PLT5-GR* promotes multiple vascular strand (A′) formation upon leaf incision and callus formation (white arrows) at cut end of detached organ (B′) unlike in mock-treated control (A,B). (C-D′) Overexpression of *35S::PLT7-GR* enhances multiple strand formation upon leaf incision (C′) and wound repair upon inflorescence abrasion (D′) unlike in mock-treated control (C,D). (E,F) Only a residual cell proliferation response is observed in *plt3;plt5-2;plt7* (E) unlike the extensive callus-like growth observed in *plt3;plt5-2;plt7;AtPLT5::OsPLT2-vYFP* (F) in response to inflorescence abrasion. Dotted rectangle indicates area of cell proliferation. (G) Expression of *AtPLT5::OsPLT2-vYFP* in vascular tissue (white arrowhead) of a *plt3;plt5-2;plt7* leaf. (H-J) Rescue of vascular tissue regeneration in response to leaf incision in *plt3;plt5-2;plt7;AtPLT5::OsPLT2-vYFP* (I,J) (***P*=0.004; Pearson's χ^2 test) compared with *plt3;plt5-2;plt7* leaves (H), of which ~61% failed to regenerate. Error bars represent s.e.m. Black arrowheads indicate incision site. Red dotted lines indicate regenerated vascular strands. Dex, dexamethasone. Scale bars: 50 µm (A,A′,C,C′,G-I); 1 mm (B,B′,D-F). D, days after injury.

PLT3,5,7 directly activate *CUC2* expression for wound repair and vascular regeneration

Having established that *PLT3,5,7* regulate wound repair and vascular regeneration in damaged aerial parts of the plant, we sought to define the molecular mechanisms underlying this regulation. Previously, we had shown that *PLT3,5,7* direct tissue-culture-mediated *in vitro* shoot regeneration by activating root stem cell regulators and *CUC2* (Kareem et al., 2015). Although we found no evidence for the participation of PLT1, PLT2 and WOX5 root stem cell regulators in the response to injuries in growing aerial organs (Figs S4 and S9A), *CUC2* remains an attractive candidate for participation in wound repair. Therefore, we investigated whether *CUC2* responds to mechanical injury and whether *PLT3,5,7* act through *CUC2* to repair wounds and regenerate vasculature.

pCUC2::3XVENUS as well as *CUC2::CUC2-vYFP* expression was detected in vascular tissue of young leaves in both wild-type and *plt3;plt5-2;plt7* mutant plants although expression was reduced in the latter (Fig. 4A,A′, Fig. S9B-F,I,I′). The same *CUC2* promoter was used to drive transcriptional and translational fusions. The detection of an expanded domain of expression of *pCUC2::3XVENUS* compared with *CUC2::CUC2-vYFP* can be largely attributed to *3XVENUS*. Both reporter fusions used in this study can recapitulate the previously reported *CUC2* expression at the leaf margin (Nikovics et al., 2006; Bilsborough et al., 2011) (Fig. S9G,H). In response to midvein damage in wild type, expression of both *pCUC2::3XVENUS* and *CUC2::CUC2-vYFP* was upregulated proximal to the wound 12 h post-injury followed by a broader domain of enhanced expression after 24 h (Fig. 4B,C, Fig. S9I-K). In contrast, there was no upregulation of the reporter near the wound site in *plt3;plt5-2;plt7* (Fig. 4B′,C′, Fig. S9I′-K′). Similar patterns of changes were also observed at the transcript level in response to midvein injury (12 h post-injury) (Fig. S9L). Similarly, in damaged inflorescence stems, *CUC2* transcripts were reduced in the *plt3;plt5-2;plt7* compared with wild type (Fig. 4D). Furthermore, *CUC2* transcripts rapidly increased in injured leaves upon inducible overexpression of PLT5 (*35S::PLT5-GR*) as well as of PLT7 (*35S::PLT7-GR*) even in the presence of the

Development (2020) 147, dev185710. doi:10.1242/dev.185710

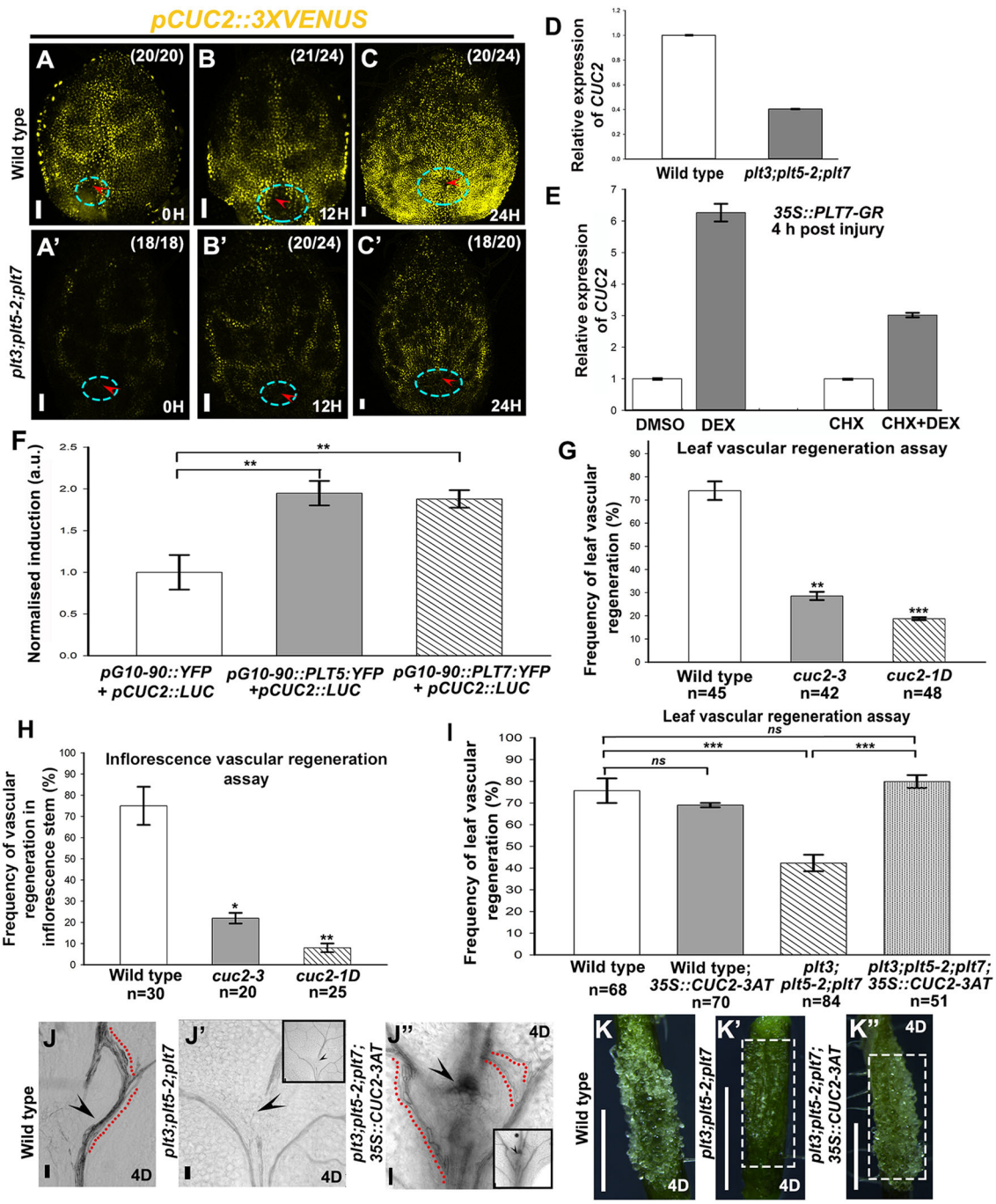

Fig. 4. *PLT* genes act through *CUC2* to repair wounds and to regenerate vascular tissue. (A-C′) Reduced expression of *pCUC2::3XVENUS* (yellow) in *plt3;plt5-2;plt7* (A′-C′) compared with wild type (A-C) in response to injury. Red arrowheads denote incision site and dashed circles enclose leaf tissue in the vicinity of the wound showing upregulation of *pCUC2::3XVENUS* in wild type but not in *plt3;plt5-2;plt7*. Sample numbers are shown in parentheses (numerator, number of samples showing the expression represented in the image panel; denominator, total number of samples analysed). (D) Relative expression levels (qRT-PCR) of *CUC2* in injured *plt3;plt5-2;plt7* mutant inflorescence segments compared with wild type (4 dpi). (E) Rapid upregulation of *CUC2* (qRT-PCR) in injured tissue upon induction of *35S::PLT7-GR*. Expression levels in D and E are normalised to *ACTIN2*. Error bars represent s.e.m. from three independent biological replicates. (F) PLT5 and PLT7 induce *pCUC2* in a luciferase reporter assay 2 days post-inoculation in *Nicotiana*. $^{**}P<0.01$ (Mann–Whitney *U* one-tailed test). Six biological replicates each with three technical replicates were performed. (G) Frequency of leaf vascular regeneration in *cuc2-3* (recessive) ($^{**}P=0.007$), *cuc2-1D* (dominant) ($^{***}P=0.0005$) mutants compared with wild type (Pearson's χ^2 test). (H) Frequency of vascular regeneration in response to partial incision in the inflorescence stem of wild type, *cuc2-3* and *cuc2-1D* ($^{*}P=0.02$, $^{**}P=0.001$; Pearson's χ^2 test). (I) Frequency of leaf vascular regeneration in wild type, wild type;*35S::CUC2-3AT* (ns, not significant; $P=0.65$), *plt3;plt5-2;plt7* ($^{***}P=9.9\times10^{-5}$) and *plt3;plt5-2;plt7;35S::CUC2-3AT* ($^{***}P=4.7\times10^{-6}$) (Pearson's χ^2 test). (J) Representative example of vascular regeneration in a wild-type leaf. (J′,J″) Vascular tissue regeneration is rescued in *plt3;plt5-2;plt7;35S::CUC2-3AT* (J″) compared with *plt3;plt5-2;plt7* (J′) in response to leaf incision (black arrowheads). Note the increased vascular strand proliferation and regeneration of multiple vascular strands (red dotted lines) generating multiple reunion points in *plt3;plt5-2;plt7;35S::CUC2-3AT* (J″) unlike in *plt3;plt5-2;plt7* (J′). Insets show the incision site. (K) Representative example of local cell proliferation response in a wild-type inflorescence stem in response to abrasion. (K′,K″) Ectopic overexpression of *CUC2* in *plt3;plt5-2;plt7* (*plt3;plt5-2;plt7;35S::CUC2-3AT*) (K″) enhances local cell proliferation and wound healing response upon inflorescence abrasion (enclosed by dashed rectangle) compared with *plt3;plt5-2;plt7* (K′). Error bars represent s.e.m. Scale bars: 1 mm (K-K″); 50 µm (A-C′,J-J″). D, days after injury; H, hours after injury.

Development (2020) 147, dev185710. doi:10.1242/dev.185710

translation inhibitor cycloheximide, suggesting direct activation of *CUC2* transcription by PLT5 and PLT7 (Fig. 4E, Fig. S9M). Consistent with these observations, PLT5 bound to the *CUC2* promoter in a chromatin immunoprecipitation (ChIP) assay (Fig. S9N). In addition, DNA affinity purification sequencing (DAP-Seq) analysis identified the binding of PLT7 to the *CUC2* promoter (O'Malley et al., 2016, http://neomorph.salk.edu/) (Fig. S10A). Furthermore, transient transfection of trans genes capable of producing PLT5 or PLT7 proteins and the *CUC2* promoter-driven luciferase reporter in *Nicotiana* leaf induced reporter expression, further demonstrating that PLT5 as well as PLT7 can directly activate *CUC2* transcription (Fig. 4F).

Because molecular data indicate that *CUC2* acts downstream of *PLT* genes, we investigated whether PLT proteins require *CUC2* activity for wound repair. Strikingly, inducible ectopic overexpression of PLT5 failed to promote wound repair at the damaged end of *cuc2-3* (*cuc2-3;35S::PLT5-GR*) mutant tissues. The severely compromised wound repair that was observed at the cut ends remained unaltered upon PLT5 overexpression in *cuc2-3* detached tissue, but not upon PLT5 overexpression in wild type (Wild type;*35S::PLT5-GR*), which enhanced wound repair at the cut ends (Fig. S10B-F). These results demonstrate that PLT proteins act through *CUC2* to repair the wound.

We examined the role of *CUC2* in leaf vascular regeneration by analysing loss-of-function mutants. Strikingly, vascular regeneration was severely impaired in both the recessive loss-of-function *cuc2-3* mutant as well as in the *cuc2-1D* dominant mutant; 71% of *cuc2-3* mutant and 81% of *cuc2-1D* mutant leaves failed to show any vascular regeneration in response to midvein injury (Fig. 4G). Notably, loss of *CUC2* function did not cause any defect in the formation of closed vein loops formed by primary (midvein) and secondary (lateral) veins (Fig. S7F,G,J,K,L). Similarly, upon inflorescence stem incision, ∼78% *cuc2-3* mutant and 92% of *cuc2-1D* mutant inflorescence stems failed to show any vascular regeneration (Fig. 4H). Finally, we asked whether *CUC2* overexpression can rescue the vascular regeneration defect in *plt3;plt5-2;plt7* mutant leaves. Strikingly, the regeneration efficiency (timings of regeneration and reunion of vascular strands) as well as frequency (number of plants) was restored upon *CUC2* overexpression in *plt3;plt5-2;plt7* to the level of wild type. New vascular strands regenerated and reunited by 4 dpi in the mutant, similar to wild type (Fig. 4I-J″). Moreover, *CUC2* overexpression rescued the repair process in locally wounded *plt3;plt5-2;plt7* inflorescence stems (Fig. 4K-K″). Taken together, these data demonstrate that *PLT3,5,7* directly activate *CUC2* transcription in response to injury and that the *PLT-CUC2* module is required for wound repair and vascular regeneration in leaf and stem. Interestingly, the growth of inflorescence stems and leaves were similar in wild type and the *cuc2-3* mutant (Fig. S5H,K).

PLT genes are required for polarised cell growth and auxin response during vascular regeneration

CUC2 is implicated in the regulation of leaf margin development by directing PIN1 polarity and the resultant auxin distribution (Bilsborough et al., 2011) and PIN1 polarisation is crucial for the normal development of leaf vasculature (Scarpella et al., 2006). Hence, we next investigated whether the process of cell polarisation is regulated by the *PLT* transcription module during leaf vascular regeneration. We focused on *in vivo* vascular regeneration in developing leaves, which has not been explored. To this end, we examined the localisation of PIN1 in response to midvein injury in the leaf blade (Fig. S11C′-F′,G′-J′). Prior to wounding, we observed *PIN1::PIN1-GFP* expression in the procambium predominantly towards the basal end of young leaves in both wild type and mutant (Fig. S11A-F,G-J). In response to injury, we observed increased PIN1-GFP near wound sites in both wild type and mutant (Fig. S11E′,I′). To examine PIN1-GFP localisation in regenerating vascular cells, we generated transgenic lines harbouring both *PIN1::PIN1-GFP* and *ATHB8::ATHB8-vYFP*. ATHB8 specifically marks developing procambium cells in leaf (Scarpella et al., 2004). We observed both PIN1-GFP and ATHB8-YFP in developing procambium of 4-day-old leaves (Fig. 5A,B).

During the first 12 h following incision, we did not observe regenerating vascular cells expressing both PIN1-GFP and ATHB8-YFP near wound sites (Fig. 5C,D). Regenerating procambium cells marked with ATHB8-YFP and polarised PIN1-GFP were observed after 24 h near wound in wild type (Fig. 5E). In contrast, we did not observe regenerating procambium cells expressing polarised PIN1-GFP or ATHB8-YFP near the wound after 24 h in *plt3;plt5-2;plt7* plants, demonstrating that cells surrounding the damaged site failed to re-specify the PIN1 polarity in the mutant (Fig. 5F). These data suggest that failure of re-establishment of polar auxin transport within 24 h may contribute to impaired vascular regeneration in the *plt* triple mutant. We next examined whether lack of directional auxin flow in the damaged *plt3;plt5-2;plt7* mutant leaves altered the distribution patterns of the auxin response. We examined the auxin response using the auxin reporter *pDR5rev::3XVENUS-N7* in both wild-type and *plt3;plt5-2;plt7* mutant plants. Prior to injury, we did not observe any difference in distribution patterns or levels of the auxin response in leaves between these two genotypes (Fig. 5G,G′, Fig. S11K-M′). In both wild type and *plt3;plt5-2;plt7* an increase in *pDR5rev::3XVENUS-N7* signal in the tissue proximal to the wound was observed at 24 h post-injury (Fig. 5H,H′,I,I′). However, a further enhanced auxin response was confined to an area near the wound site by 48 h only in wild type (Fig. 5J). In contrast to wild type, the triple mutant failed to show such confined expression of *pDR5rev::3XVENUS-N7* signal in response to injury (Fig. 5J′). The distribution patterns and levels of auxin response in uninjured developing mutant leaves compared with wild type did not change, further substantiating the specific role of *PLT3,5,7* in response to injury (Fig. 5G,G′, Fig. S11K-M′). Taken together, our results show that PLT3,5,7 are needed for re-specification of polarised vascular cells to facilitate vascular tissue regeneration.

PLT proteins and CUC2 activate the transcription of local auxin biosynthesis gene in a feed-forward loop to repair wounds and drive vascular regeneration

Local auxin biosynthesis has been implicated in root haustoria formation and associated vascular development during host-parasite interaction (Kokla and Melnyk, 2018). We therefore asked whether PLT-CUC2 module regulate wound repair and vascular regeneration by modulating local auxin biosynthesis genes. Interestingly, local auxin biosynthesis genes are downregulated in *plt3;plt5-2;plt7* mutant callus (A.K. and K.P., unpublished data). PLT proteins are also known to control phyllotaxis by regulating one of the auxin biosynthesis genes, *YUCCA4* (*YUC4*) (Pinon et al., 2013). Similarly, *YUC4* expression was upregulated in response to midvein injury (12 h post-injury) in growing wild-type leaves, unlike in the *plt3;plt5-2;plt7* leaves, in which the transcript level was reduced (Fig. 6A). In addition to damaged leaves, *YUC4* transcripts were also reduced in damaged *plt3;plt5-2;plt7* inflorescence segments (Fig. S12A). Conversely, *YUC4* transcripts were rapidly increased in injured tissues upon PLT5-GR induction (4 h) even in the presence of the translation inhibitor cycloheximide, suggesting direct activation by

Development (2020) 147, dev185710. doi:10.1242/dev.185710

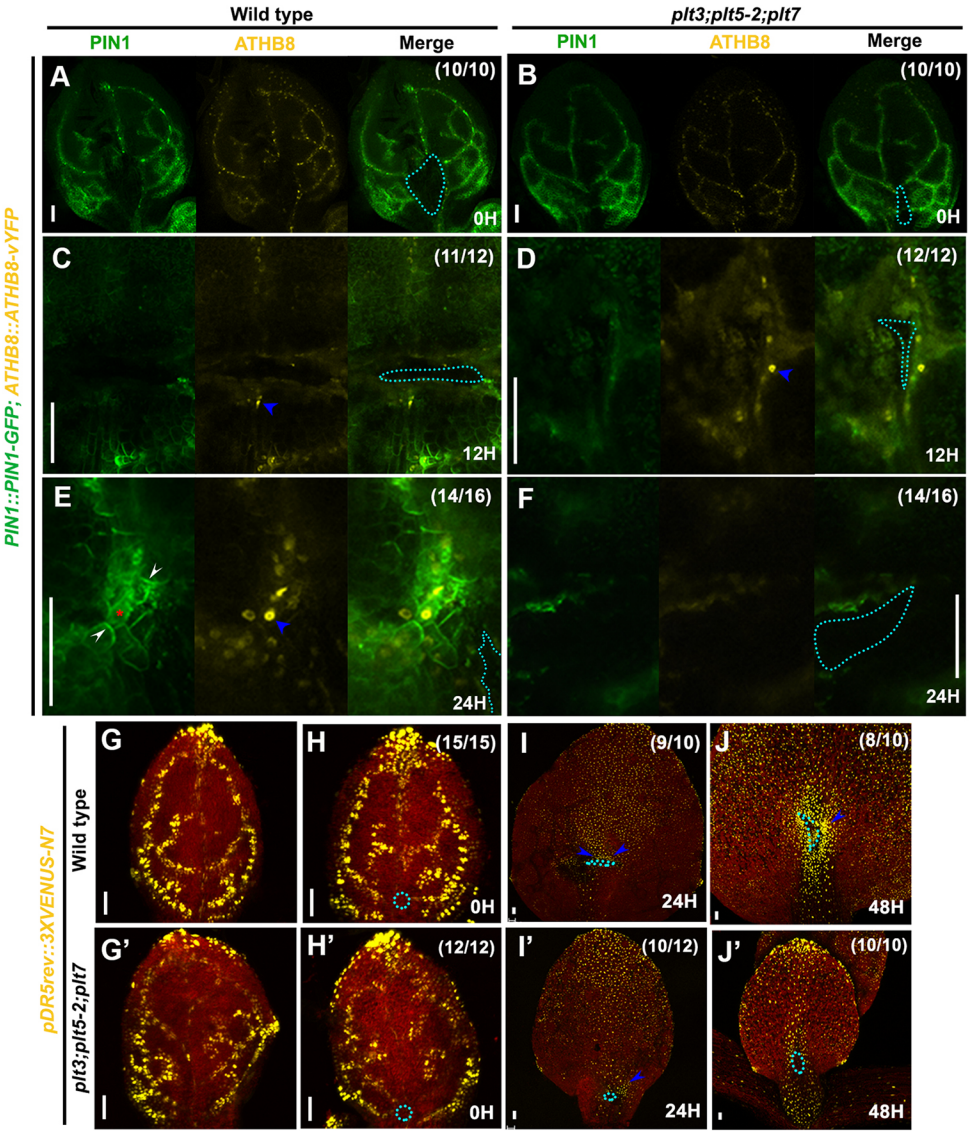

Fig. 5. *PLT* genes regulate polarised cell growth and auxin response during vascular regeneration. (A-F) Expression of *PIN1::PIN1-GFP* and *ATHB8::ATHB8-vYFP* in wild-type (A,C,E) and *plt3;plt5-2;plt7* mutant (B,D,F) leaves in response to leaf incision. (A,B) YFP channel shows expression of *ATHB8::ATHB8-vYFP* in procambium cells of the leaf. (C,D) No expression of PIN1 is detected in the immediate vicinity of the wound at 12 h in either wild type (C) or *plt3;plt5-2;plt7* (D). Pre-existing ATHB8 (blue arrowheads) expression is observed near the wound (in C and D YFP channel). (E,F) Expression of polarised *PIN1::PIN1-GFP* (white arrowheads) and *ATHB8::ATHB8-vYFP* (blue arrowhead) in the regenerating cells (hexagonal developing procambium cells; indicated by red asterisk) of wild type. PIN1 polarisation and ATHB8 expression is absent in *plt3;plt5-2;plt7* (F). Blue dotted area indicates tissue damaged by leaf incision. Brightness of YFP channel (representing ATHB8) signal was increased for visibility in A-F. A-F show a subset of *z*-stack sections. (G,G′) *pDR5rev::3XVENUS-N7* expression in undamaged leaves of wild type (G) and *plt3;plt5-2;plt7* (G′). (H-J′) *pDR5rev::3XVENUS-N7* expression in wild-type (H-J) and *plt3;plt5-2;plt7* (H′-J′) leaves post-incision (dotted area indicates incision site). *plt* mutant leaf remains small due to stunted growth following injury. Note the confined expression of *pDR5rev::3XVENUS-N7* in the tissue around the wound (blue arrowheads) in wild type (J) unlike in *plt3;plt5-2;plt7* (J′). Scale bars: 50 µm. Red colour in G-J′ represents chlorophyll autofluorescence. Sample numbers are shown in parentheses (numerator, number of samples showing the expression represented in the image panel; denominator, total number of samples analysed). H, hours after injury.

PLT5 (Fig. 6B). Because molecular data suggests that *YUC4* acts downstream of *PLT* genes, we investigated whether PLT proteins require *YUC4* activity to trigger cellular reprogramming. Strikingly, inducible overexpression of PLT5 as well as PLT7 failed to trigger any ectopic cellular reprogramming in the *yuc4;yuc1* mutant background (*yuc4;yuc1;35S::PLT5-GR* or *yuc4;yuc1;35S::PLT7-GR*), unlike in the wild-type background (Wild type;*35S::PLT5-GR*; or Wild type;*35S::PLT7-GR*) (Fig. S12B,C). Similarly, PLT5 as well as PLT7 overexpression failed to promote wound repair at damaged ends, demonstrating that PLT proteins act through *YUC4* during reprogramming and wound repair (Fig. S12D-G).

We explored whether, in addition to *PLT* genes, *CUC2* might also contribute towards regulating the local auxin biosynthesis in response to injury. *YUC4* transcripts were not upregulated in response to midvein injury in the *cuc2-1D* single mutant (Fig. 6A) and its transcript levels were rapidly increased upon *CUC2-GR* induction even in the presence of the translation inhibitor cycloheximide, suggesting direct activation of *YUC4* expression by CUC2 (Fig. 6C). Consistent with the likelihood of direct activation of *YUC4* transcription by CUC2 inferred from our results, DAP-Seq analysis indicated the binding of CUC2 to the *YUC4* promoter (Fig. S12H) (O'Malley et al., 2016, http://neomorph.salk.edu/). Next, we examined whether, like PLT proteins, CUC2 also requires downstream *YUC4* activity to promote vascular regeneration. Ectopic overexpression of CUC2 promoted vascular regeneration in the leaf and resulted in regeneration of multiple vascular strands from the wound site in the wild type (Wild type;*35S::CUC2-3AT*) (Fig. 6D). In contrast to wild type, ectopic overexpression of CUC2 failed to promote regeneration of multiple vascular strands from the wound site in the *yuc4;yuc1* mutant (*yuc4;yuc1;35S::CUC2-3AT*) (Fig. 6D-F). Injured leaves in *yuc4;yuc1;35S::CUC2-3AT* seedlings either did not regenerate any vascular strand or occasionally displayed a single file of regenerating vascular cells as was observed in *yuc4;yuc1* (Fig. 6E,F, Fig. S12I). These data demonstrate that, like *PLT* genes, *CUC2* also acts through *YUC4* to promote wound repair and vascular regeneration.

Our data suggest that, in addition to PLT proteins, CUC2 can also activate *YUC4* expression during vascular regeneration. Activation of *YUC4* by PLT5, PLT7 and CUC2 indicates a feed-forward loop controlling local auxin biosynthesis (Fig. 6B,C, Fig. S12J). *PLT5-GR* can only moderately activate *YUC4* expression after 4 h induction when the function of *CUC2* and of the redundantly acting *CUC1* is lost (in damaged *cuc1-5;cuc2-3* tissues) (Fig. 6H), indicating that increased transcription of *YUC4* in wild-type damaged leaves may be

Development (2020) 147, dev185710. doi:10.1242/dev.185710

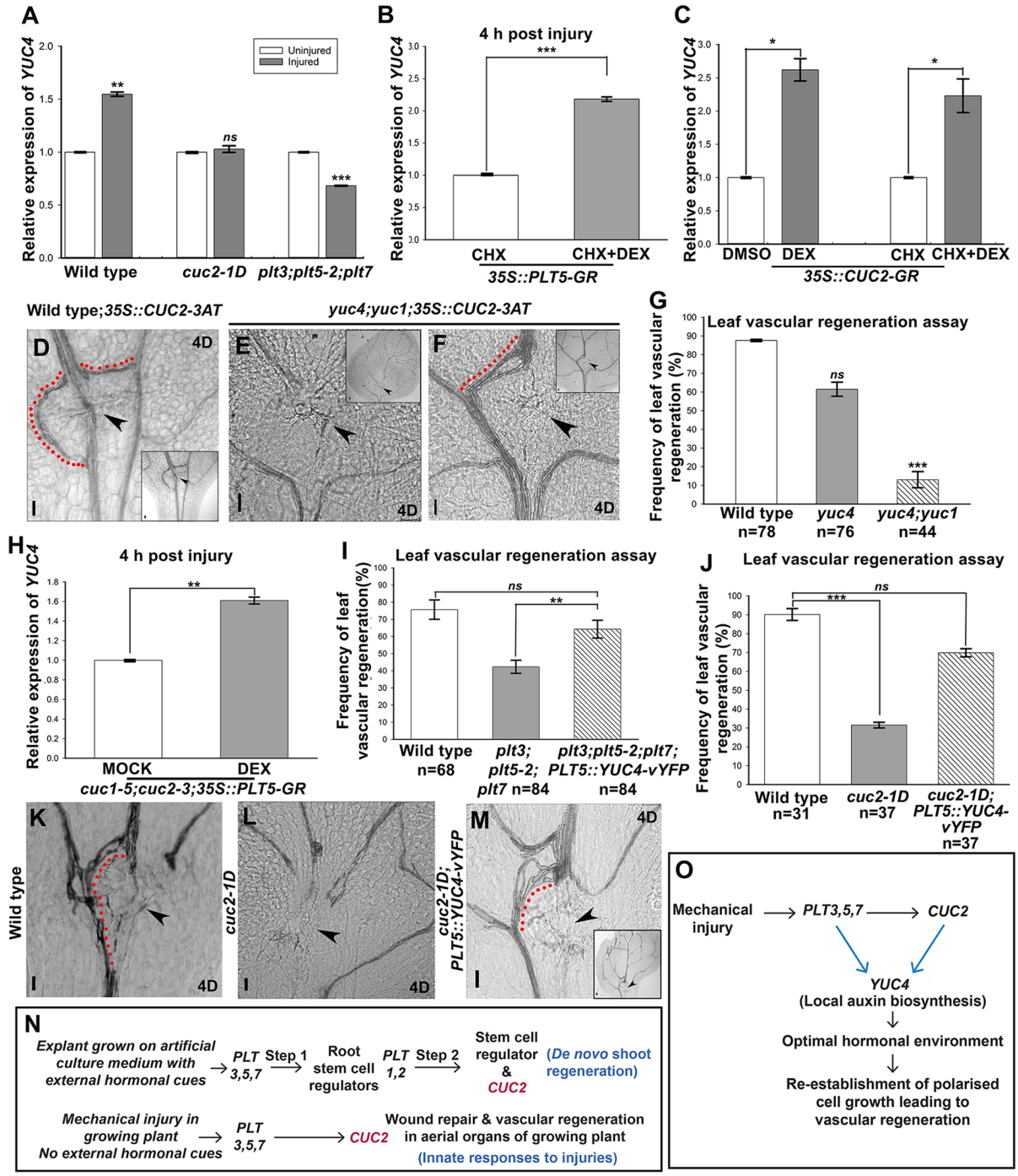

Fig. 6. *PLT*- and *CUC2*-dependent auxin biosynthesis drives vascular regeneration in leaf. (A) *YUC4* transcript level in wild-type, *cuc2-1D* and *plt3;plt5-2;plt7* injured and uninjured leaves, measured by qRT-PCR (ns, not significant, P=0.45; **P=0.001, ***P=0.0002; Welch's two-sample *t*-test). (B) Upregulation of *YUC4* (qRT-PCR) transcript level in injured leaves upon induction of *35S::PLT5-GR* with cycloheximide (CHX) treatment (***P=0.0008; Welch's two-sample *t*-test). (C) Upregulation of *YUC4* (qRT-PCR) transcript levels in injured leaves upon induction of *35S::CUC2-GR* with and without CHX treatment (*P<0.05; Welch's two-sample *t*-test). (D-F) Ectopic overexpression of CUC2 produced multiple vascular strands from the wound site in wild type;*35S::CUC2-3AT* (D) unlike in *yuc4;yuc1;35S::CUC2-3AT* (E,F). (G) Percentage of leaf vascular regeneration in wild type, *yuc4* (ns, not significant; P=0.8) and *yuc4;yuc1* (***P=1.02×10^{-6}; Pearson's χ^2 test).(H) *YUC4* transcript level in *cuc1-5;cuc2-3* upon induction of *35S::PLT5-GR*, measured by qRT-PCR. Data shown in A-C,H are normalised to *ACTIN2*. Error bars represent s.e.m. from three independent biological replicates (**P=0.0032; Welch's two-sample *t*-test). (I) Frequency of leaf vascular regeneration in wild type, *plt3;plt5-2;plt7* (ns, not significant, P=0.18) and *plt3;plt5-2;plt7;PLT5::YUC4-vYFP* (**P=0.0087, Pearson's χ^2 test). (J-M) Reconstitution of local auxin biosynthesis gene in the *PLT5* domain rescues leaf vascular regeneration in the *cuc2-1D* mutant (***P=4.11×10^{-6}; ns, not significant, P=0.08). Error bars represent s.e.m. Black arrowheads indicate incision site. Red dotted lines indicate regenerated vascular strands. Insets in D-F,M show lower magnification images of the site of injury. Scale bars: 50 µm. D, days after injury. (N) Schematic showing the *PLT-CUC2* module independently activating innate regeneration responses to injuries, which is unlike the sequential activation of CUC2 after activation of root stem cell regulators during *de novo* shoot regeneration. (O) Schematic representing the mechanistic module of PLT transcription factors activating *CUC2* and *YUC4* to generate an optimal auxin environment to aid in re-establishment of polarised growth of vascular cells. Regulatory interactions marked using light blue arrows emerged from the present study and were not known previously in any regeneration context.

Development (2020) 147, dev185710. doi:10.1242/dev.185710

an output of a coherent feed-forward loop during tissue regeneration. We further provide genetic evidence for the feed-forward loop: inducible overexpression of PLT7 or PLT5 can still increase vascular regeneration by 18% and 24%, respectively, in response to midvein injury in the *cuc2-3* mutant (Fig. S12K).

We further investigated this regulatory interaction by analysing the genetic interaction between *PLT* genes and *CUC2*. Strikingly, we found synergistic interaction between *PLT* genes and *CUC2* during wound repair and vascular regeneration. Cumulative loss of PLT and CUC2 function in the *plt3;plt5-2;plt7;cuc2-3* mutant resulted in severely compromised wound repair at the cut end of the detached plant organ compared with the *plt3;plt5-2;plt7* or *cuc2-3* mutant (Fig. S13A). In addition to dramatically reduced frequency of wound repair in *plt3;plt5-2;plt7;cuc2-3* mutant, we could barely observe any proliferating callus-like cells at the damaged ends in *plt3;plt5-2;plt7;cuc2-3* mutant organs (Fig. S13B-E). The *YUC4* transcript level was further reduced in the *plt3;plt5-2;plt7;cuc2-3* mutant compared with the *plt3;plt5-2;plt7* or *cuc2-3* mutant (Fig. S13F). Similarly, seedlings heterozygous for *plt* and *cuc2* alleles, $plt3^{+/-};plt5\text{-}2^{+/-};plt7^{+/-};cuc2\text{-}3^{+/-}$ displayed hypersensitivity to leaf midvein injury compared with $plt3^{+/-};plt5\text{-}2^{+/-};plt7^{+/-}$ or $cuc2\text{-}3^{+/-}$ (Table S1, Fig. S7L). These data substantiate the regulation of YUC4 expression by PLT proteins and CUC2 in a coherent feed-forward loop during wound repair and vascular regeneration.

Consistent with the importance of activation of *YUC4* expression for regeneration, ∼40% of *yuc4* single mutant and 87% of *yuc4;yuc1* double mutant leaves failed to regenerate vascular tissue in response to midvein injury (Fig. 6G). Strikingly, the uninjured *yuc4* single mutant develops a fully grown midvein without any discontinuity and there is no significant difference in the formation of closed vein loops compared with wild type (Fig. S7F,G,M). Although midvein formation in the *yuc4;yuc1* mutant was normal, as in the wild type, the number of loops surrounding the midvein was reduced (Fig. S7F,G,N). Strikingly, reconstitution of *YUC4* expression in the endogenous *PLT5* domain (*PLT5::YUC4-vYFP*) in the *plt3;plt5-2;plt7* mutant as well as in the *cuc2-1D* mutant rescued the vascular regeneration in injured leaves to a large extent (Fig. 6I-M, Fig. S13G-I). These data provide compelling evidence for the functional significance of *PLT-CUC2* module-dependent activation of local auxin biosynthesis in controlling vascular regeneration. Remarkably, reconstitution of *YUC4* expression in the *cuc1-5;cuc2-3* (*cuc1-5;cuc2-3;PLT5::YUC4-vYFP*) mutant, which generates cup-shaped cotyledons but no leaf or stem, rescued post-embryonic development with fully developed rosette leaves (Fig. S14).

DISCUSSION

Multicellular organisms display the ability to regrow damaged tissues and organs. Unlike many animals, in which regeneration potential is restricted to specific cell lineages, plants repair and rebuild damaged tissues throughout the body. In this study, we have investigated the mechanism of wound repair across aerial parts of the plant body, identifying PLT/AIL transcription factors, well known for their role in stem cell maintenance, as regulatory triggers for this process. We demonstrate that activation of *CUC2* transcription by PLT3,5,7 is a key regulatory mechanism of wound repair and vascular regeneration: (1) PLT factors bind to the *CUC2* promoter and directly activate the transcription of *CUC2*; (2) PLT factors require downstream CUC2 activity during wound repair; and (3) reconstitution of CUC2 expression under a heterologous promoter in *plt3;plt5-2;plt7* triple mutants rescues vascular regeneration. We provide evidence that PLT proteins and CUC2 activate the transcription of local auxin biosynthesis gene in a feed-forward loop to drive vascular regeneration: (1) both PLT and CUC2 require downstream YUC4 activity as ectopic overexpression of PLT proteins as well as of CUC2 fails to trigger regeneration response in the *yuc4;yuc1* mutant; (2) reconstitution of YUC4 expression under a heterologous promoter in the *plt* triple mutant as well as in the *cuc2-1D* mutant rescues the vascular regeneration defects; and (3) PLT proteins and CUC2 act synergistically to activate *YUC4* transcription and repair the damaged tissues, which involves induction of vascular identity and proper polarisation of the polar auxin transporter PIN1.

Our study revealed a previously unrecognised role of *ANT* in vascular regeneration and demonstrated that a *PLT*-like gene from rice, a morphologically diverse grass species, could substitute the regeneration function of *Arabidopsis PLT* genes. These observations indicate that the activation of *PLT* gene promoters in response to mechanical injuries may be more important for the selection of regeneration-associated *PLT* genes than their protein sequence. In this context, it is relevant that distinct PLT transcription factors determine competence for regeneration in the root context (Durgaprasad et al., 2019).

In striking contrast to *in vitro* shoot regeneration cues (Kareem et al., 2015), *PLT3,5,7* do not act through the root stem cell regulators PLT1, PLT2 and WOX5 to initiate repair of damaged aerial tissues of a growing plant. Rather, PLT proteins act through *CUC2* by directly activating its expression (Fig. 6N). Interestingly, *PLT* genes and *CUC2* act in a feed-forward loop to activate the expression of the auxin biosynthesis gene *YUC4* (Fig. 6O). This circuit can act as a coherent feed-forward loop, which often serves as a signal persistence detector (Mangan et al., 2003), even though our analysis indicates that the regulatory logic at the promoter is not strictly an 'AND gate' (Alon, 2006). Regardless of the precise regulatory logic, the output of the circuit is the activation of YUC4. In that view, it is tantalising that the cellular defects associated with the malfunctioning of this circuit are the inability to redirect ground tissue cells to vascular identity and the inability to properly polarise PIN proteins. A regulatory feedback loop between auxin level, auxin flux and polarisation of auxin efflux carriers (PIN) has been proposed as a key regulatory mechanism of shoot branching, phyllotaxis and vascular tissue differentiation (Jönsson et al., 2006; Smith et al., 2006; Bayer et al., 2009; Schuetz et al., 2012; Mazur et al., 2016; Fujita and Kawaguchi, 2018). It is therefore conceivable that *PLT-CUC2*-dependent activation of *YUC4* activates this feedback loop to drive vascular regeneration in damaged growing leaves (Fig. 6O). In summary, our study reveals *PLT-CUC2* regulatory axis is specifically involved in controlling regeneration through induction of a local hormonal environment in response to injury.

MATERIALS AND METHODS

Plant materials

Arabidopsis thaliana ecotype Columbia (Col-0) was used as wild type in this study. The origins of the mutants used in the study, such as the double mutants *plt3;plt5-2*, *plt3;plt7* and *plt5-2;plt7* and the triple mutant *plt3;plt5-2;plt7* (Prasad et al., 2011), the double mutant *yuc4;yuc1* (Pinon et al., 2013), the single mutant *ant-4*, double mutant *ant-4;plt5-3* and the triple mutant *plt3;plt7;ant-4* (Krizek, 2015), the single mutants *cuc2-1D* (Larue et al., 2009) and *cuc2-3* (Hibara et al., 2006), and the double mutant *cuc1-5;cuc2-3* (Hibara et al., 2006), have been described previously. Translational fusion constructs of *PLT1::PLT1-vYFP*, *PLT2::PLT2-vYFP* (Mähönen et al., 2014), *PLT3::PLT3-vYFP*, *PLT5::PLT5-vYFP* and *PLT7::PLT7-vYFP* (Prasad et al., 2011) have been described previously. *35S::PLT5-GR, 35S::PLT7-GR* (Prasad et al., 2011), *pCUC2::3XVENUS* and *35S::CUC2-3AT* (Kareem et al., 2015) have been described previously. Multisite gateway recombination cloning system

Development (2020) 147, dev185710. doi:10.1242/dev.185710

(Invitrogen) using the pCAMBIA 1300 destination vector was used for cloning the translational fusion constructs, which were then introduced into the C58 *Agrobacterium* strain by electroporation and further transformed into wild-type or mutant *Arabidopsis* plants by the floral dip method (Clough and Bent, 1998) (see supplementary Materials and Methods for details on plasmid construction). *DR5rev::3XVENUS-N7* expression was examined in wild-type and *plt3;plt5-2;plt7* transgenic plants with the double marker *pDR5rev::3XVENUS-N7,PIN1::PIN1-GFP* line, which has been described previously (Pinon et al., 2013). In this study, only the YFP marker was analysed using a single YFP channel.

Growth conditions

Arabidopsis thaliana seeds were surface sterilised with 70% ethanol and 20% bleach, followed by seven washes with sterile distilled water. Seeds were plated on half-strength Murashige-Skoog (MS) medium (pH 5.7) and grown vertically under 45 µmol/m^2/s continuous white light at 22°C and 70% relative humidity.

Regeneration assays

For wound-induced natural regeneration experiments, all plants and explants were grown on hormone-free half-strength MS agar medium (Sigma-Aldrich). To study wound repair and vascular regeneration in growing inflorescence stems, 3-week-old seedlings were selected. Using a sterile razor blade, the stem region between the rosette leaves and the first or second cauline leaves was subjected to either peeling of the tissue layers including epidermis and sub epidermal layers (inflorescence abrasion) or partial incision (inflorescence incision) through the vascular tissues under a dissection microscope (Zeiss Stemi 2000). The observations were recorded 4 days after wounding. For the leaf vascular regeneration assay, to maintain uniformity we injured a single leaf belonging to the first pair of rosette leaves of 5 dpg seedlings. Plants of same developmental stage were chosen for incision. Fine-pointed sterile tweezers (Dumont tweezer, Style 5) were used to make a sharp incision in the midvein at the basal part of the leaf blade. To avoid ambiguity, incisions made elsewhere were not scored. The incisions were made from the abaxial surface of the leaf to ensure precise injury to the midvein. The injured leaf was left connected to the growing parent plant and it was protected from any further damage. Vascular regeneration was analysed in the injured leaf 4 days post-incision. These leaves were cut at the petiole using Vannas straight scissors (Ted Pella, 1340) without causing additional damage to the leaf blade. The leaf tissue was cleared using chloral hydrate (Sigma-Aldrich) (see supplementary Materials and Methods for further details of decolourisation and tissue clearing) and brightfield images were obtained to assess the regeneration outcomes. When newly formed vascular strands (identified by the distinct morphology of end-to-end connected xylem elements) connected the cut ends of the midvein to form a D-shaped loop or connected the damaged midvein to a lateral vein, the outcomes were scored as successful regeneration (Fig. 2I,J). To study healing in response to wounding in excised organs (leaf/root), excised explants were collected from 9 dpg seedlings and placed on hormone-free MS agar medium. Upon excision, continuous dexamethasone (Sigma-Aldrich) induction was provided until the tenth day post-excision for samples collected from transgenic lines harbouring steroid-inducible constructs. The corresponding mock-treated samples were incubated on MS plates containing an equal proportion of DMSO (same volume as dexamethasone). The plates were kept in the dark for the first 24-32 h and later shifted to continuous light. All the plates of regeneration experiments were incubated vertically in a plant growth chamber maintained at 22°C and 70% relative humidity under 45 µmol/m^2/s continuous white light.

Microscopic imaging

Brightfield and confocal laser-scanning microscopy imaging were performed as described previously (Kareem et al., 2015). Brightfield images of vascular regeneration in incised leaves were acquired using the brightfield mode in a Leica TCS SP5 II inverted confocal microscope and an Olympus BX63F fluorescence microscope after clearing the leaf sample (see supplementary Materials and Methods for details of decolourisation and tissue clearing). Confocal imaging of leaves and thick samples were performed using a Leica TCS SP5 II upright microscope and a Zeiss LSM 880 confocal laser-scanning microscope. Brightfield images acquired using Leica M205 FA fluorescence stereo microscope and confocal microscopes were adjusted for brightness and contrast. For confocal imaging, the cell boundaries of inflorescence stem samples were stained using 10 µg/ml propidium iodide (Sigma-Aldrich). Images were acquired using 10× air, 20× oil immersion, 20× air and 40× oil immersion objectives. The projection view of the images was reconstructed from the *z*-stacks with Leica LAS-AF software and Zeiss ZEN blue softwares. Images were compiled using Adobe Photoshop CS6 and Adobe Photoshop CC 2015. All image panels represent *z*-stacks unless mentioned. The area of callus formation at the cut end of detached organs was measured using ImageJ software.

qRT-PCR

Total RNA was extracted from samples (see supplementary Materials and Methods for further details of sample preparation) using the Nucleospin Plant RNA extraction kit (MN) and subjected to on-column DNase treatment according to the manufacturer's guidelines. cDNA was synthesised from 1 µg total RNA using a High-Capacity cDNA Reverse Transcription kit (Applied Biosystems). qRT-PCR was performed in a 25 µl reaction volume containing 12.5 µl SYBR Green PCR master mix (Takara Bio), 100 nM gene-specific primers (Table S1) and 100 ng cDNA in a CFX96 Touch Real-Time PCR Detection System. All reactions were performed with RNA derived from three independent biological replicates. Each biological sample was tested in technical triplicate. Data were normalised to *ACTIN2* (*ACT2*). The transcript level in the control was normalised to 1. The expression of the gene of interest is represented with respect to the control (as performed by Kareem et al., 2015). The relative gene expression is represented as fold-change value by calculating $-\Delta\Delta C^T$.

Luciferase assay

The luciferase assay was performed as described by Díaz-Triviño et al. (2017). Healthy *Nicotiana benthamiana* plants (3-4 weeks old) grown under long-day conditions (16 h light, 8 h dark) were used for agroinfiltration. The primers used for cloning are listed in Table S2. Competent cells of the C58 strain of *Agrobacterium tumefaciens* were used for the infiltration.

ChIP-qPCR analysis

ChIP was performed by following the protocol as described by Yamaguchi et al. (2014) (see supplementary Materials and Methods for a brief description). ChIP-qPCR was performed using SYBR Premix (Clontech) to determine PLT5 protein occupancy on the *CUC2* promoter region. The relative fold enrichment of CUC2 DNA was calculated by computing the enrichment in *PLT5::PLT5-vYFP* relative to *plt3;plt5-2;plt7*. *ACTIN7* (*ACT7*) was used to normalise the results between the samples. The ChIP-qPCR reactions were performed in triplicate. The primers used for ChIP-qPCR are listed in Table S3.

Statistical analysis

Pearson's χ^2 test (regeneration assay analysis), Welch's two-sample *t*-test (qRT-PCR data analysis), Mann–Whitney *U* one-tailed test (luciferase assay) and Kruskal–Wallis χ^2 test (comparing the number of closed vein loops) were used for data analysis. The Holm–Bonferroni correction was performed for multiple analysis when using Pearson's χ^2 test. R programming was used for the statistical analyses.

Acknowledgements

We thank Dr Philip N. Benfey, Dr Elliot Meyerowitz and Dr Ottoline Leyser for their valuable suggestions on the early draft of the manuscript. We are grateful to Dr Charles Melnyk and Dr Utpal Nath for all the discussions and help. *pG10-90:vYFP* control vector for luciferase assay was received from Menno Pijnenburg. We are thankful to M. R. Krishna Prashanth for assistance with schematics and figures, B. Subhiksha for cloning *AtPLT5::OsPLT2-vYFP* and Sajesh Vijayan for help with the statistical analyses.

Competing interests

The authors declare no competing or financial interests.

Author contributions

Conceptualization: D.R., A.K., K.P.; Methodology: D.R., A.P.S., A.K., M.A., V.V., A.T., M.K., D.V., A.N.L., V.W., K.P.; Formal analysis: D.R., A.P.S., A.K., M.A., A.T.,

A.S., M.K.M., V.W., B.S., K.P.; Investigation: A.K., K.P.; Resources: A.K., M.G.S., E.S., B.A.K., I.E., A.P.M., B.S., K.P.; Writing - original draft: D.R., A.K.; Writing - review & editing: D.R., A.P.S., A.T., B.S., K.P.; Visualization: D.R., A.P.S., A.K., K.P.; Supervision: K.P.; Funding acquisition: K.P.

Funding

K.P. acknowledges grants from the Department of Biotechnology (DBT), Government of India [grant BT/PR12394/AGIII/103/891/2014] and Department of Science and Technology, Science and Engineering Research Board (DST-SERB), Government of India [grant EMR/2017/002503/PS] and also acknowledges the Indian Institute of Science Education and Research Thiruvananthapuram (IISER-TVM) for infrastructure and financial support. D.R. acknowledges a University Grants Commission (UGC) fellowship. A.P.S., V.V. and A.T. are recipients of Council of Scientific and Industrial Research (CSIR) fellowships. A.K. was supported by an Indian Institute of Science Education and Research-Thiruvananthapuram fellowship. M.A. acknowledges Department of Biotechnology (DBT), Ministry of Science and Technology, Government of India for granting the DBT-Post Doctoral Fellowship (DBT-RA Program). D.V. was a recipient of an Innovation in Science Pursuit for Inspired Research scholarship, and A.N.L was supported by a Kishore Vaigyanik Protsahan Yojana scholarship of the Department of Science and Technology, Government of India. A.P.M. acknowledges grants from the Academy of Finland [grants 266431 and 271832]. I.E. acknowledges the Israel Science Foundation [ISF966/17] and the Howard Hughes Medical Institute [International Research Scholar Grant 55008730]. B.A.K. was supported by a grant from National Science Foundation (NSF) [grant NSFIOS135442]. E.S. was supported by Discovery Grants of the Natural Science and Engineering Research Council of Canada [grants NSERC RGPIN-2016-04736 and NSERC RGPAS 492872-2016].

Data availability

All raw data associated with this article have been deposited in Mendeley (https://data.mendeley.com/datasets/mwyxw4v63h/draft?a=e64505aa-564b-4127-9d0c-afc900810544).

Supplementary information

Supplementary information available online at
http://dev.biologists.org/lookup/doi/10.1242/dev.185710.supplemental

Peer review history

The peer review history is available online at
https://dev.biologists.org/lookup/doi/10.1242/dev.185710.reviewer-comments.pdf

References

Alon, U. (2006). *An Introduction to Systems Biology*. New York: Chapman and Hall/CRC.

Asahina, M., Azuma, K., Pitaksaringkarn, W., Yamazaki, T., Mitsuda, N., Ohme-Takagi, M., Yamaguchi, S., Kamiya, Y., Okada, K., Nishimura, T. et al. (2011). Spatially selective hormonal control of RAP2.6L and ANAC071 transcription factors involved in tissue reunion in Arabidopsis. *Proc. Natl. Acad. Sci. USA* **108**, 16128-16132. doi:10.1073/pnas.1110443108

Bayer, E. M., Smith, R. S., Mandel, T., Nakayama, N., Sauer, M., Prusinkiewicz, P. and Kuhlemeier, C. (2009). Integration of transport-based models for phyllotaxis and midvein formation. *Genes Dev.* **23**, 373-384. doi:10.1101/gad.497009

Bilsborough, G. D., Runions, A., Barkoulas, M., Jenkins, H. W., Hasson, A., Galinha, C., Laufs, P., Hay, A., Prusinkiewicz, P. and Tsiantis, M. (2011). Model for the regulation of Arabidopsis thaliana leaf margin development. *Proc. Natl. Acad. Sci. USA* **108**, 3424-3429. doi:10.1073/pnas.1015162108

Clough, S. J. and Bent, A. F. (1998). Floral dip: a simplified method for Agrobacterium-mediated transformation of Arabidopsis thaliana. *Plant J.* **16**, 735-743. doi:10.1046/j.1365-313x.1998.00343.x

Díaz-Triviño, S., Long, Y., Scheres, B. and Blilou, I. (2017). Analysis of a plant transcriptional regulatory network using transient expression systems. In *Methods in Molecular Biology* (ed. K. Kaufmann and B. Mueller-Roeber), pp. 83-103: Humana Press.

Donner, T. J., Sherr, I. and Scarpella, E. (2009). Regulation of preprocambial cell state acquisition by auxin signaling in Arabidopsis leaves. *Development* **136**, 3235-3246. doi:10.1242/dev.037028

Du, Y. and Scheres, B. (2017). PLETHORA transcription factors orchestrate de novo organ patterning during Arabidopsis lateral root outgrowth. *Proc. Natl. Acad. Sci. USA* **114**, 11709-11714. doi:10.1073/pnas.1714410114

Durgaprasad, K., Roy, M. V., Venugopal, M. A., Kareem, A., Raj, K., Willemsen, V., Mähönen, A. P., Scheres, B. and Prasad, K. (2019). Gradient expression of transcription factor imposes a boundary on organ regeneration potential in plants. *Cell Rep.* **29**, 453-463.e3. doi:10.1016/j.celrep.2019.08.099

Efroni, I., Mello, A., Nawy, T., Ip, P.-L., Rahni, R., DelRose, N., Powers, A., Satija, R. and Birnbaum, K. D. (2016). Root regeneration triggers an embryo-like sequence guided by hormonal interactions. *Cell* **165**, 1721-1733. doi:10.1016/j.cell.2016.04.046

Flaishman, M. A., Loginovsky, K. and Lev-Yadun, S. (2003). Regenerative xylem in inflorescence stems of Arabidopsis thaliana. *J. Plant Growth Regul.* **22**, 253-258. doi:10.1007/s00344-003-0030-y

Fujita, H. and Kawaguchi, M. (2018). Spatial regularity control of phyllotaxis pattern generated by the mutual interaction between auxin and PIN1. *PLoS Comput. Biol.* **14**, e1006065. doi:10.1371/journal.pcbi.1006065

Galliot, B., Crescenzi, M., Jacinto, A. and Tajbakhsh, S. (2017). Trends in tissue repair and regeneration. *Development* **144**, 357-364. doi:10.1242/dev.144279

Hibara, K.-I., Karim, M. R., Takada, S., Taoka, K.-I., Furutani, M., Aida, M. and Tasaka, M. (2006). Arabidopsis CUP-SHAPED COTYLEDON3 regulates postembryonic shoot meristem and organ boundary formation. *Plant Cell* **18**, 2946-2957. doi:10.1105/tpc.106.045716

Ikeuchi, M., Ogawa, Y., Iwase, A. and Sugimoto, K. (2016). Plant regeneration: cellular origins and molecular mechanisms. *Development* **143**, 1442-1451. doi:10.1242/dev.134668

Ikeuchi, M., Shibata, M., Rymen, B., Iwase, A., Bågman, A.-M., Watt, L., Coleman, D., Favero, D. S., Takahashi, T., Ahnert, S. E. et al. (2018). A gene regulatory network for cellular reprogramming in plant regeneration. *Plant Cell Physiol.* **59**, 765-777. doi:10.1093/pcp/pcy013

Jönsson, H., Heisler, M. G., Shapiro, B. E., Meyerowitz, E. M. and Mjolsness, E. (2006). An auxin-driven polarized transport model for phyllotaxis. *Proc. Natl. Acad. Sci. USA* **103**, 1633-1638. doi:10.1073/pnas.0509839103

Kareem, A., Durgaprasad, K., Sugimoto, K., Du, Y., Pulianmackal, A. J., Trivedi, Z. B., Abhayadev, P. V., Pinon, V., Meyerowitz, E. M., Scheres, B. et al. (2015). PLETHORA genes control regeneration by a two-step mechanism. *Curr. Biol.* **25**, 1017-1030. doi:10.1016/j.cub.2015.02.022

Kokla, A. and Melnyk, C. W. (2018). Developing a thief: haustoria formation in parasitic plants. *Dev. Biol.* **442**, 53-59. doi:10.1016/j.ydbio.2018.06.013

Krizek, B. A. (2015). AINTEGUMENTA-LIKE genes have partly overlapping functions with AINTEGUMENTA but make distinct contributions to Arabidopsis thaliana flower development. *J. Exp. Bot.* **66**, 4537-4549. doi:10.1093/jxb/erv224

Larue, C. T., Wen, J. and Walker, J. C. (2009). A microRNA-transcription factor module regulates lateral organ size and patterning in Arabidopsis. *Plant J.* **58**, 450-463. doi:10.1111/j.1365-313X.2009.03796.x

Mähönen, A. P., Ten Tusscher, K., Siligato, R., Smetana, O., Díaz-Triviño, S., Salojärvi, J., Wachsman, G., Prasad, K., Heidstra, R. and Scheres, B. (2014). PLETHORA gradient formation mechanism separates auxin responses. *Nature* **515**, 125. doi:10.1038/nature13663

Mangan, S., Zaslaver, A. and Alon, U. (2003). The coherent feedforward loop serves as a sign-sensitive delay element in transcription networks. *J. Mol. Biol.* **334**, 197-204. doi:10.1016/j.jmb.2003.09.049

Marhava, P., Hoermayer, L., Yoshida, S., Marhavý, P., Benková, E. and Friml, J. (2019). Re-activation of stem cell pathways for pattern restoration in plant wound healing. *Cell.* **177**, 957-969.e13. doi:10.1016/j.cell.2019.04.015

Mazur, E., Benková, E. and Friml, J. (2016). Vascular cambium regeneration and vessel formation in wounded inflorescence stems of Arabidopsis. *Sci. Rep.* **6**, 33754. doi:10.1038/srep33754

Melnyk, C. W., Schuster, C., Leyser, O. and Meyerowitz, E. M. (2015). A developmental framework for graft formation and vascular reconnection in Arabidopsis thaliana. *Curr. Biol.* **25**, 1306-1318. doi:10.1016/j.cub.2015.03.032

Nikovics, K., Blein, T., Peaucelle, A., Ishida, T., Morin, H., Aida, M. and Laufs, P. (2006). The balance between the MIR164A and CUC2 genes controls leaf margin serration in Arabidopsis. *Plant Cell* **18**, 2929-2945. doi:10.1105/tpc.106.045617

Ohashi-Ito, K., Oguchi, M., Kojima, M., Sakakibara, H. and Fukuda, H. (2013). Auxin-associated initiation of vascular cell differentiation by LONESOME HIGHWAY. *Development* **140**, 765-769. doi:10.1242/dev.087924

O'Malley, R. C., Huang, S.-C., Song, L., Lewsey, M. G., Bartlett, A., Nery, J. R., Galli, M., Gallavotti, A. and Ecker, J. R. (2016). Cistrome and epicistrome features shape the regulatory DNA landscape. *Cell* **165**, 1280-1292. doi:10.1016/j.cell.2016.04.038

Pinon, V., Prasad, K., Grigg, S. P., Sanchez-Perez, G. F. and Scheres, B. (2013). Local auxin biosynthesis regulation by PLETHORA transcription factors controls phyllotaxis in Arabidopsis. *Proc. Natl. Acad. Sci. USA* **110**, 1107-1112. doi:10.1073/pnas.1213497110

Pitaksaringkarn, W., Matsuoka, K., Asahina, M., Miura, K., Sage-Ono, K., Ono, M., Yokoyama, R., Nishitani, K., Ishii, T., Iwai, H. et al. (2014). *XTH20* and *XTH19* regulated by ANAC071 under auxin flow are involved in cell proliferation in incised Arabidopsis inflorescence stems. *Plant J.* **80**, 604-614. doi:10.1111/tpj.12654

Prasad, K., Grigg, S. P., Barkoulas, M., Yadav, R. K., Sanchez-Perez, G. F., Pinon, V., Blilou, I., Hofhuis, H., Dhonukshe, P., Galinha, C. et al. (2011). Arabidopsis PLETHORA transcription factors control phyllotaxis. *Curr. Biol.* **21**, 1123-1128. doi:10.1016/j.cub.2011.05.009

Radhakrishnan, D., Kareem, A., Durgaprasad, K., Sreeraj, E., Sugimoto, K. and Prasad, K. (2018). Shoot regeneration: a journey from acquisition of competence to completion. *Curr. Opin. Plant Biol.* **41**, 23-31. doi:10.1016/j.pbi.2017.08.001

Reinhardt, D., Frenz, M., Mandel, T. and Kuhlemeier, C. (2003). Microsurgical and laser ablation analysis of interactions between the zones and layers of the tomato shoot apical meristem. *Development* **130**, 4073-4083. doi:10.1242/dev.00596

Sachs, T. (1968). On the determination of the pattern of vascular tissue in peas. *Ann. Bot.* **32**, 781-790. doi:10.1093/oxfordjournals.aob.a084249
Sachs, T. (1969). Polarity and the induction of organized vascular tissues. *Ann. Bot.* **33**, 263-275. doi:10.1093/oxfordjournals.aob.a084281
Sachs, T. (1981). The control of the patterned differentiation of vascular tissues. In *Advances in Botanical Research* (ed. H. W. Woolhouse), pp. 151-262: Academic Press.
Sachs, T. (1991). *Pattern Formation in Plant Tissues*. New York: Cambridge University Press.
Scarpella, E., Francis, P. and Berleth, T. (2004). Stage-specific markers define early steps of procambium development in Arabidopsis leaves and correlate termination of vein formation with mesophyll differentiation. *Development* **131**, 3445-3455. doi:10.1242/dev.01182
Scarpella, E., Marcos, D., Friml, J. and Berleth, T. (2006). Control of leaf vascular patterning by polar auxin transport. *Genes Dev.* **20**, 1015-1027. doi:10.1101/gad.1402406
Schuetz, M., Smith, R. and Ellis, B. (2012). Xylem tissue specification, patterning, and differentiation mechanisms. *J. Exp. Bot.* **64**, 11-31. doi:10.1093/jxb/ers287
Smetana, O., Mäkilä, R., Lyu, M., Amiryousefi, A., Sánchez Rodríguez, F., Wu, M. F., Solé-Gil, A., Leal Gavarrón, M., Siligato, R., Miyashima, S. et al. (2019). High levels of auxin signalling define the stem-cell organizer of the vascular cambium. *Nature* **565**, 485-489. doi:10.1038/s41586-018-0837-0
Smith, R. S., Guyomarc'h, S., Mandel, T., Reinhardt, D., Kuhlemeier, C. and Prusinkiewicz, P. (2006). A plausible model of phyllotaxis. *Proc. Natl. Acad. Sci. USA* **103**, 1301-1306. doi:10.1073/pnas.0510457103
van den Berg, C., Willemsen, V., Hage, W., Weisbeek, P. and Scheres, B. (1995). Cell fate in the Arabidopsis root meristem determined by directional signalling. *Nature* **378**, 62-65. doi:10.1038/378062a0
Wenzel, C. L., Schuetz, M., Yu, Q. and Mattsson, J. (2007). Dynamics of MONOPTEROS and PIN-FORMED1 expression during leaf vein pattern formation in Arabidopsis thaliana. *Plant J.* **49**, 387-398. doi:10.1111/j.1365-313X.2006.02977.x
Xu, J., Hofhuis, H., Heidstra, R., Sauer, M., Friml, J. and Scheres, B. (2006). A molecular framework for plant regeneration. *Science* **311**, 385-388. doi:10.1126/science.1121790
Yamaguchi, N., Winter, C. M., Wu, M. F., Kwon, C. S., William, D. A. and Wagner, D. (2014). PROTOCOL: Chromatin Immunoprecipitation from Arabidopsis Tissues. *Arabidopsis Book* **12**, e0170. doi:10.1199/tab.0170
Zhou, W., Lozano-Torres, J. L., Blilou, I., Zhang, X., Zhai, Q., Smant, G., Li, C. and Scheres, B. (2019). A jasmonate signaling network activates root stem cells and promotes regeneration. *Cell* **177**, 942-956.e14. doi:10.1016/j.cell.2019.03.006

SUPPLEMENTARY FIGURES

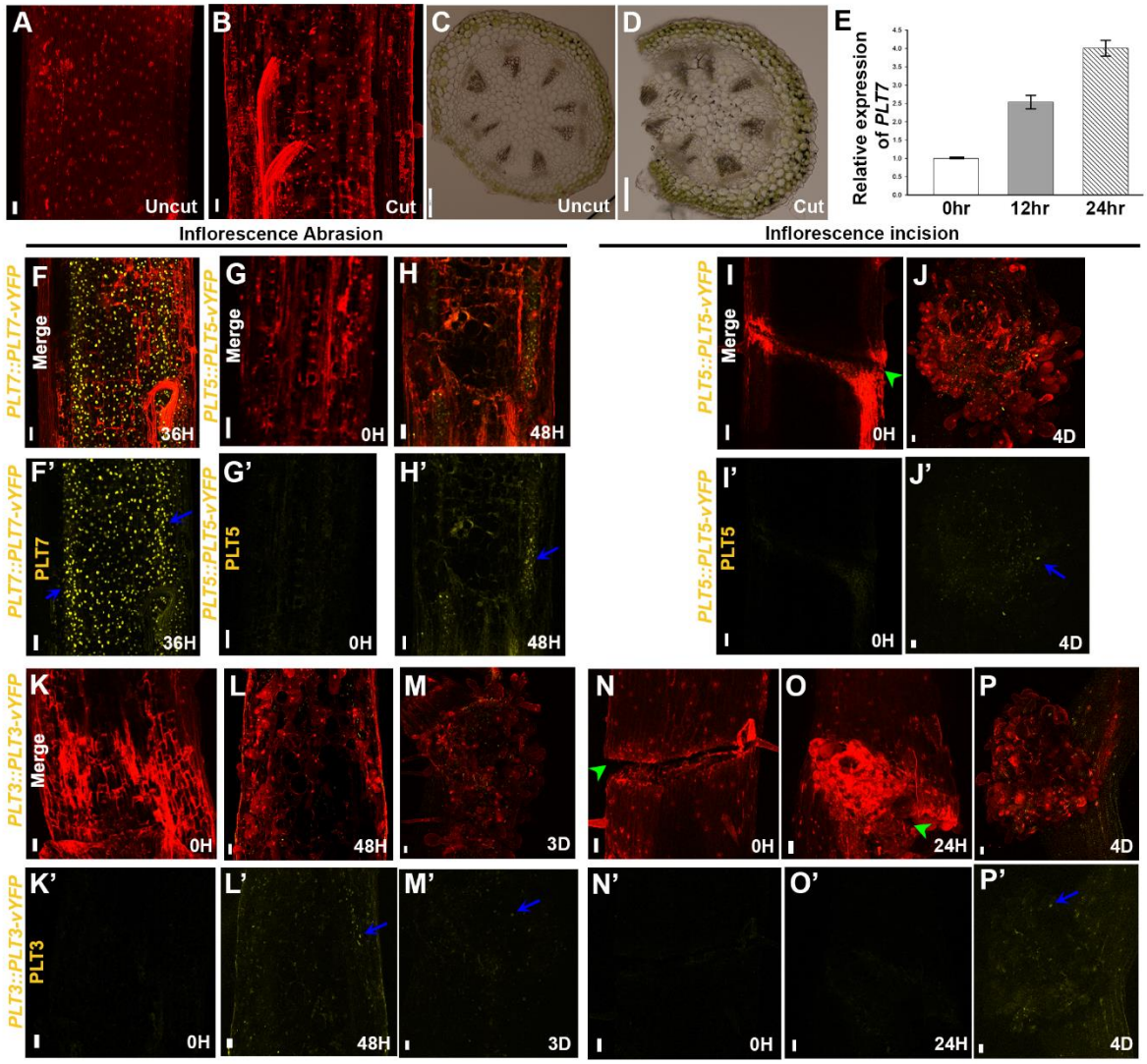

Figure S1: Dynamic expression of PLT in response to inflorescence stem injury

Inflorescence stem abrasion causes damage to epidermal and vascular tissues: (A, C) Undamaged inflorescence stem. (B, D) Sections revealing damaged epidermis and sub-epidermal layers including vascular tissue post inflorescence stem abrasion. A and B represent longitudinal sections. C and D represent transverse sections. Red colour in A, B is propidium iodide staining.

PLT7 transcript level in wild type upon partial incision in inflorescence stem: (E) Injured inflorescence stem segment encompassing the narrow domain on either side of partial slit were

collected at 0 h, 12 h and 24 h. Expression levels are normalized to *ACTIN2*. Error bar represents s.e.m. from three independent biological replicates.

PLT proteins show dynamic expression in growing aerial organs during wound healing: (F, F') Expression of *PLT7::PLT7-vYFP* in response to inflorescence stem abrasion. Note the expression of *PLT7::PLT7-vYFP* in sub-epidermal tissues and near vascular tissue (blue arrow). (G-J') Expression of *PLT5::PLT5-vYFP* during natural regeneration. Response to inflorescence stem abrasion (G-H') and inflorescence stem partial incision (green arrowhead) (I-J'). Note the increase in expression of *PLT5::PLT5-vYFP* in wounded vascular tissue in H' (blue arrow). (J') Weak expression of *PLT5::PLT5-vYFP* in callus formed in response to injury. (K-P') Expression of *PLT3::PLT3-vYFP* during natural regeneration. Response to inflorescence stem abrasion (K-M, K'-M') and inflorescence stem partial incision (N-P,N'-P'). Weak expression of *PLT3::PLT3-vYFP* is observed in sub-epidermal tissues (L') and in the callus formed in response to wounding (M' and P').

(F'-J' and K'-P'): maximum intensity projection of z stack in YFP channel corresponding to (F-J and K-P). Red colour represents propidium iodide staining. Green arrowheads: partial incision in inflorescence stem. Blue arrows: Expression of *PLT* in response to wounding. Scale bar: 50 µm except in C and D where scale bars represent 1 mm. Brightness of YFP channel has been increased in H', J', L', M' and P' for visibility. The panels (F-P) represent different samples at each time point.

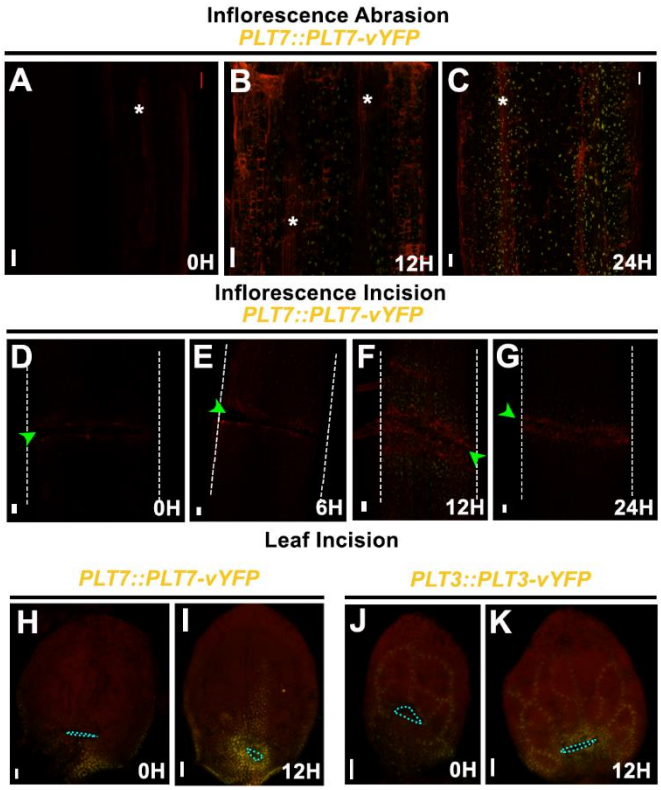

Figure S2: *PLT3, PLT5* and *PLT7* genes are locally induced after mechanical injury

(A-G) *PLT7::PLT7-vYFP* expression (yellow) post abrasion (A-C) and partial incision (green arrowhead) (D-G) in growing inflorescence stems. White asterisks: vascular tissues exposed by damage to epidermal and sub-epidermal layers following local abrasion. White dashed line: Inflorescence stem outline. (H-K) Upregulation of *PLT7::PLT7-vYFP* (H, I) and *PLT3::PLT3-vYFP* (J, K) (yellow) near wound site following leaf incision (blue dotted area: incision site). The panels represent average intensity projections of merged panels in Fig. 1 and each panel represent different samples at each time point. Red signal is propidium iodide staining in (A-G) and chlorophyll autofluoroscence in (H-K). Scale bars:50 μm.

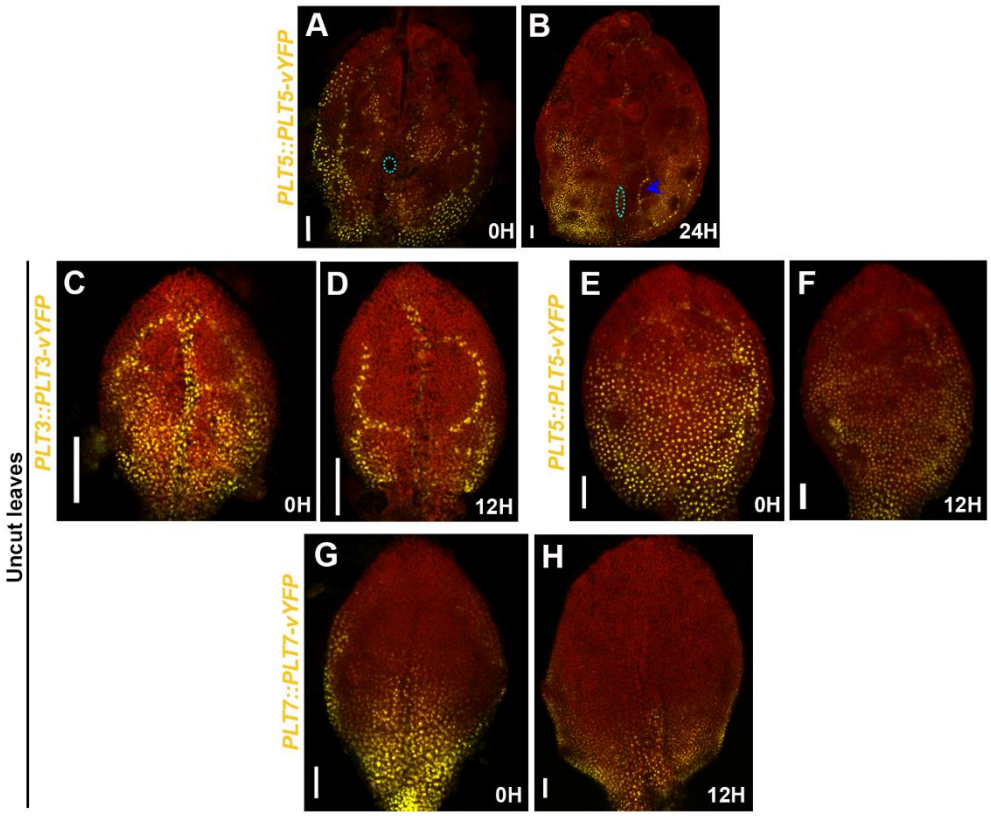

Figure S3: PLT expression in injured and undamaged leaves

(A, B) *PLT5::PLT5-vYFP* expression in adjacent vascular strand (blue arrowhead) post incision (B).

(C-H) Expression of *PLT3::PLT3-vYFP*(C, D), *PLT5::PLT5-vYFP* (E, F), *PLT7::PLT7-vYFP* (G, H), in wild type undamaged leaves.

Red colour represents chlorophyll autofluorescence. B represents a subset of z stack. Brightness and contrast have been adjusted in chlorophyll autofluorescence channel for clarity of injured part. Blue dotted area: site of incision. Scale bars: 50 μm.

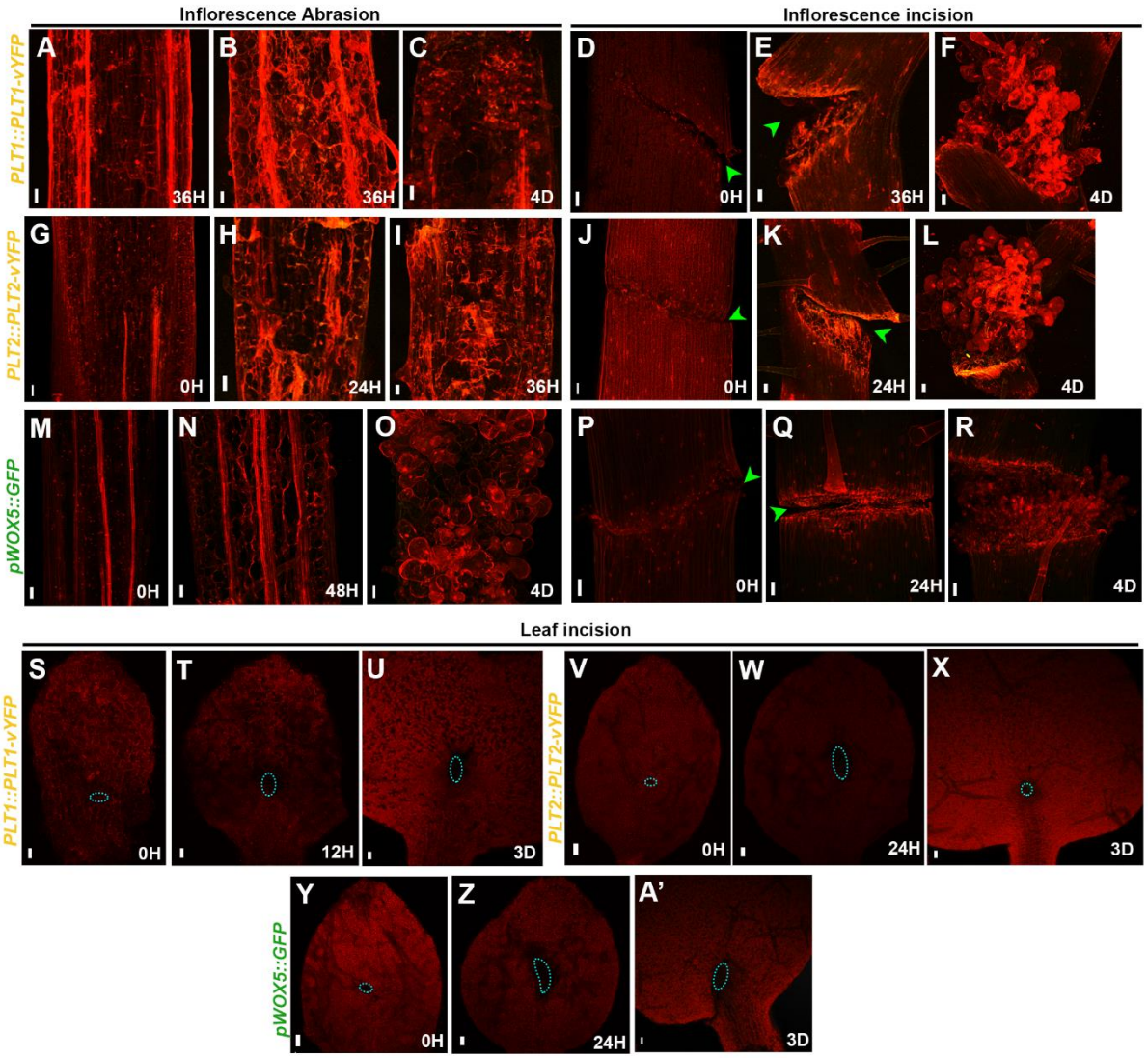

Figure S4: Absence of root stem cell regulators during wound repair in aerial organs

(A-A') Absence of *PLT1::PLT1-vYFP* (A-F, S-U), *PLT2::PLT2-vYFP* (G-L, V-X) and *pWOX5::GFP* (M-R, Y-A') following injury in growing aerial organs. Red colour in (S-A') represent chlorophyll autofluorescence and propidium iodide staining in the rest. Green arrowheads: partial incision in inflorescence stems. Blue dotted area: incision sites. Scale bars: 50 μm. Brightness and contrast have been adjusted in propidium iodide channel for clarity.

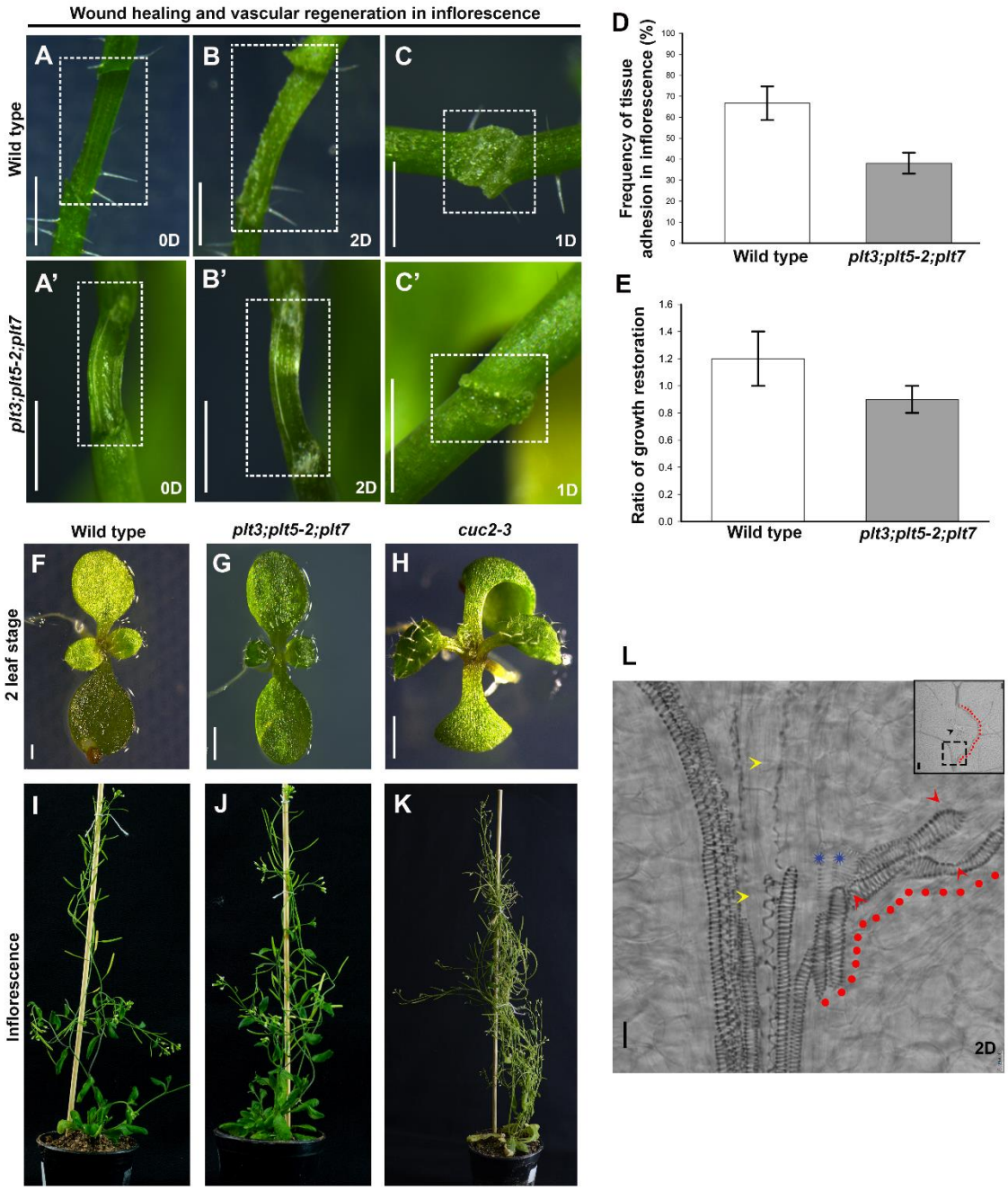

Figure S5: PLT activate innate regenerative responses to injuries in aerial organs growing in normal developmental context

(A, A') Inflorescence stem abrasion in wild type (A) and *plt3;plt5-2;plt7* (B). (B, B') Wild type inflorescence stem with cell proliferation (B) while *plt3;plt5-2;plt7* (B') inflorescence stem failed to show any proliferation. (C, C', D) More callus formation in wild type (C) 24 h following partial incision on inflorescence stem leading to increased frequency of tissue adhesion (D) in wild type as compared to *plt3;plt5-2;plt7* (C'). Dotted rectangle: area of

inflorescence stem damage. (E) Graph representing growth restoration in wild type and *plt3;plt5-2;plt7* post partial incision in inflorescence stem.

(F-K) Mutants do not display defect in the normal growth of leaves and inflorescence stems as compared to wild type.

(L) Zoomed in image shows lower cut end of midvein, two days post leaf incision. Yellow arrowheads mark degenerating vascular strands at lower cut end of midvein. Blue star: initiation of procambium differentiation into vascular cells. Red arrowheads: differentiated xylem vessel elements formed in response to injury. Red dots indicate regenerating vascular stand. Inset shows lower magnification image with black arrow marking site of leaf incision. Area enclosed in dashed line within inset is enlarged in (L).

Scale bar:1 mm in all panels except L (Scale bar: 50 μm). Error bars represent s.e.m. in all cases.

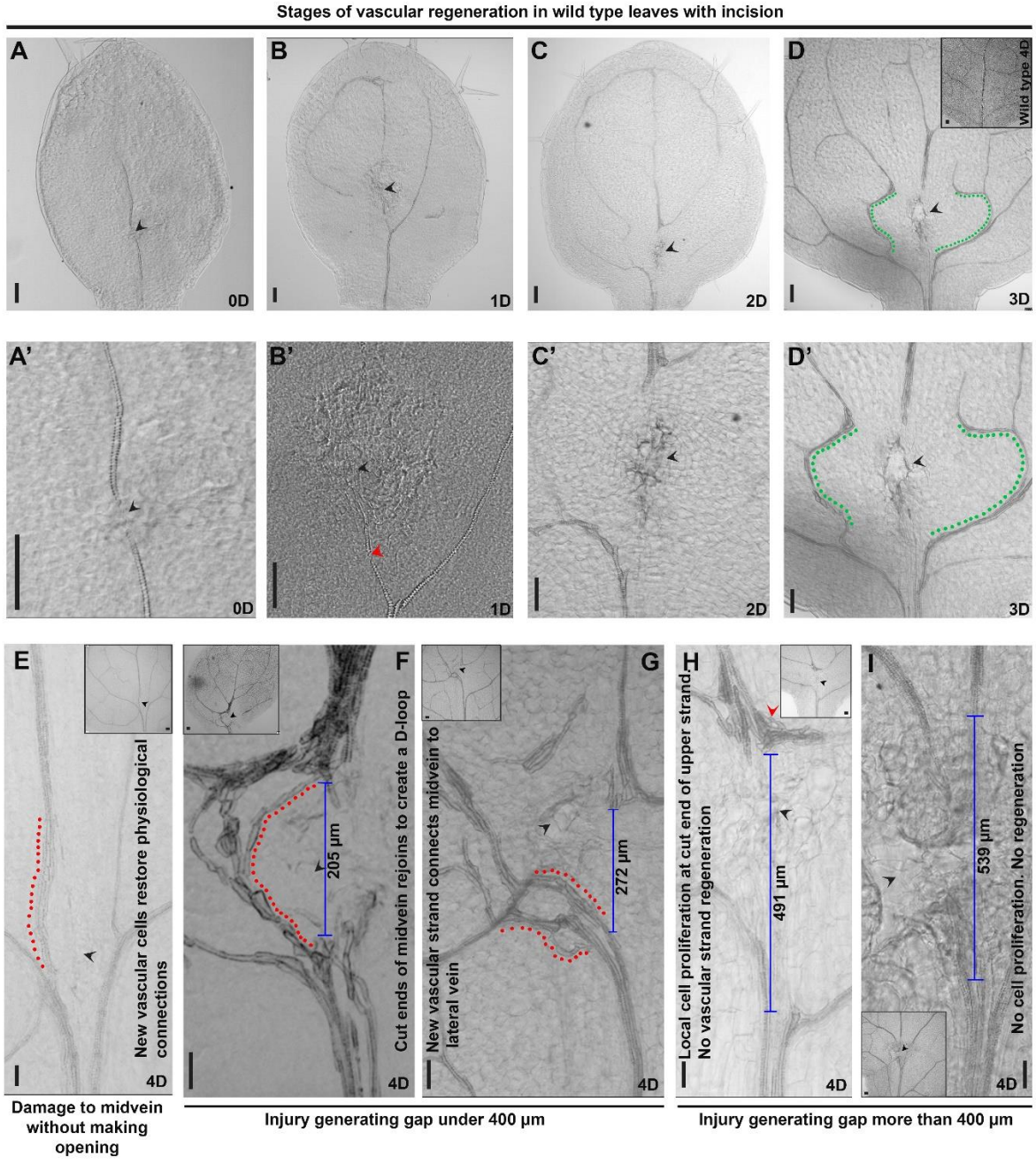

Figure S6: Response to midvein injury in leaf is dependent on the extent of tissue damage

(A-D') Stages of vascular regeneration in wild type leaves with incision: (A, A') Incision (black arrow) in midvein of 5 dpg old wild type leaf. Note that only midvein is differentiated at this stage. (B, B') Wild type leaf with incision on midvein 1 day post injury. Red arrow head: degenerating vascular strand. (C, C') Wild type leaf with incision on midvein 2 days post injury. (D, D') Wild type leaf with incision on the midvein 3 days post injury. New vascular cells form between lateral veins creating a venation pattern (green dots) which does not occur in uninjured wild type leaf (inset). (A'-D') Higher magnification images of panels

corresponding to (A-D).

(E-I) Responses to midvein injury in growing leaf. (E) Regeneration of new vascular cells (red dotted line) restore physiological connection in midvein. (F) Regenerating vascular strands (red dotted lines) rejoins disconnected ends of midvein by creating a D shaped loop (G) Regenerating vascular strands rejoins lower cut end of midvein to lateral vein. (H) Local cell proliferation (red arrow) at the cut end of upper strand but no regeneration of vascular strands. (I) No vascular cell proliferation or regeneration due to extensive area of damage creating opening in the leaf. Insets: Lower magnification images showing site of incision. Black arrowheads: Site of incision.

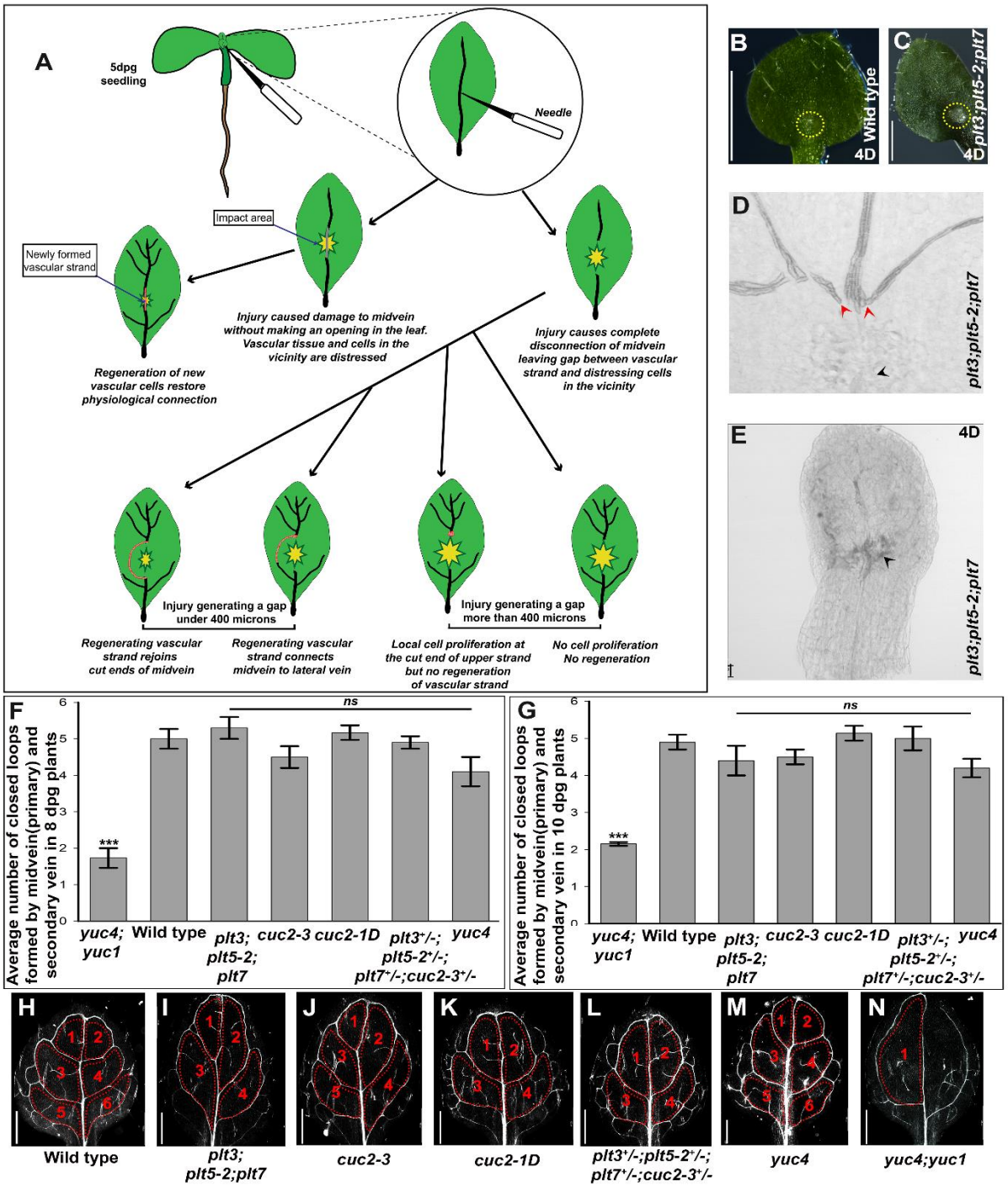

Figure S7: Normal development of vein loops in wild type and mutants

(A) Schematic representation showing vascular regeneration in response to injuries of varying sizes in the midvein of growing leaf.

(B-D) No local cell proliferation was observed on wild type leaf surface (B). Proliferation in epidermis (C) and vascular strand (D) (red arrowhead) of *plt3;plt5-2;plt7* following leaf incision (site of incision marked by yellow dotted circle/ black arrowhead).

(E) Following incision many of the *plt3;plt5-2;plt7* mutant leaves display stunted growth and slower development. Black arrowhead: site of incision.

(F, G) Number of vein loops formed by primary and secondary veins showing continuity of formation of midvein and lateral veins during normal development of first pair of wild type and mutant leaves (collected from 8 dpg and 10 dpg plants). (8 dpg samples: Kruskal–Wallis $\chi 2$ test; *P* value: *plt3;plt5-2;plt7*=0.7; *cuc2-3*=0.3; *cuc2-1D*=0.6; *plt3*$^{+}$*/-;plt5-2*$^{+}$*/-;plt7*$^{+}$*/-;cuc2-3*$^{+}$*/-*=0.8; *yuc4=0.06; yuc4;yuc1*=2x10^{-16}) (10 dpg samples: Kruskal–Wallis $\chi 2$ test*; P* value: *plt3;plt5-2;plt7*=0.2; *cuc2-3*=0.3; *cuc2-1D*=0.5; *plt3*$^{+}$*/-;plt5-2*$^{+}$*/-;plt7*$^{+}$*/-;cuc2-3*$^{+}$*/-*=0.8; *yuc4*=0.35; *yuc4;yuc1*=3.5x10^{-14}).

(H-N) Venation pattern in leaves of wild type and mutants: Mutants (except negative control-*yuc4;yuc1*) does not show significant change in formation of closed vein loops compared with wild type leaves. Red dotted lines and numbers mark closed vein loops formed by primary vein (midvein) and secondary vein (lateral vein).

Error bars represent s.e.m. in all cases.

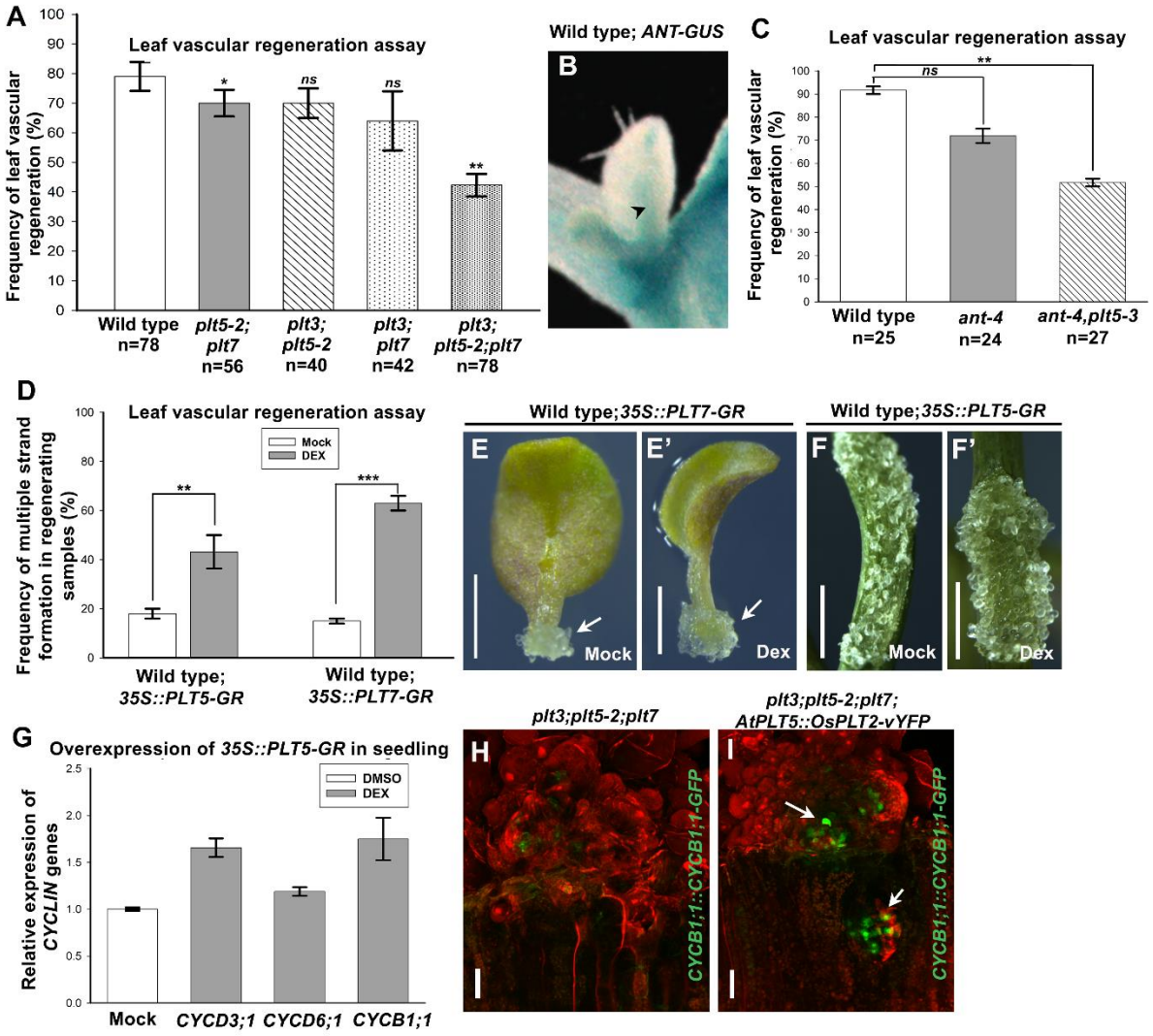

Figure S8: PLT5 and PLT7 are sufficient to promote multiple strand formation during vascular regeneration and wound repair.

(A) Frequency of leaf vascular regeneration in wild type, *plt* double mutants and *plt3;plt5-2;plt7* triple mutants (Pearson's $\chi 2$ test ;**P* =0.025;***P* =0.008;ns, *P* >0.05).

(B) Expression of *AINTEGUMENTA* in leaf vasculature (black arrow).

(C) Frequency of leaf vascular regeneration in wild type, *ant4* mutant and *ant4;plt5-3* double mutant (Pearson's $\chi 2$ test; ns, *P* >0.05;***P* =0.004).

(D) Increased multiple strand formation upon overexpression of *35S::PLT5-GR* and *35S::PLT7-GR* during vascular regeneration in response to midvein incision (Pearson's $\chi 2$ test ;***P* =0.007; ****P* =1.2x10^{-5}). (E, E') Increased callus formation (white arrow) from cut end of leaf on ectopic induction of *35S::PLT7-GR* (E') as compared to control (E). (F, F') Increased callus formation on the surface of inflorescence stem following abrasion and induction of *35S::PLT5-GR* (F') as compared to control (F). Error bars in A, C and D represent s.e.m.

(G) Expression of *CYCLIN* genes in response to overexpression of *35S::PLT5-GR* in growing

seedlings. Expression levels are normalized to *ACTIN2*. Error bar represents s.e.m. from three independent biological replicates.

(H, I) *plt3;plt5-2;plt7* (H) barely shows any cell proliferation marked by cell cycle progression marker *CYCB1;1::CYCB1;1-GFP* as compared to strong expression detected in clusters (white arrow) of actively dividing cells forming callus in response to inflorescence stem abrasion in *plt3;plt5-2;plt7;AtPLT5::OsPLT2-vYFP* (I). Confocal imaging was performed only for GFP excitation and emission detection.

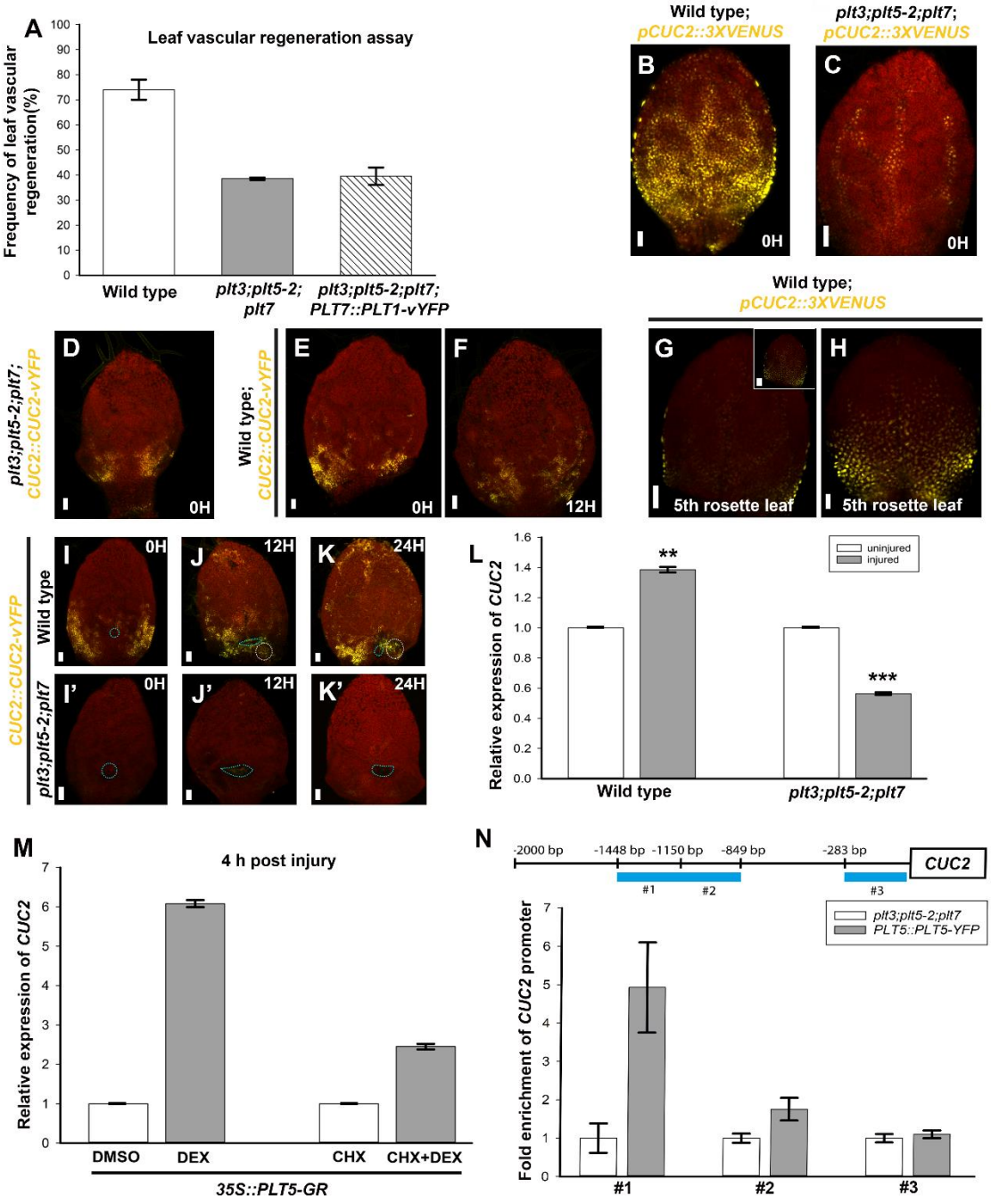

Figure S9: PLT directly activates CUC2 during wound response

(A) Leaf vascular regeneration in wild type, *plt3;plt5-2;plt7* and *plt3;plt5-2;plt7;PLT7::PLT1-vYFP*

(B-H) Expression of *CUC2* in undamaged leaves. Expression of *pCUC2::3XVENUS* (B,C) and *CUC2::CUC2-vYFP* (D-F) in undamaged leaves. (G) Single optical section showing expression of *pCUC2::3XVENUS* in the leaf margin of fifth rosette leaf. Inset in (G) represents stacked image of the same leaf. (H) *pCUC2::3XVENUS* expression is absent from the hydathode and higher in the leaf sinus as reported previously (Nikovics *et al.*, 2006;

Bilsborough *et al.*, 2011). Except (G) and (H) (5th rosette leaves), all other panels present leaves belonging to 1st pair of rosette leaves.

(I, I') *plt3;plt5-2;plt7* shows reduced expression of *CUC2::CUC2-vYFP* as compared to wild type.

(J-K') Upon incision wild type (J,K) shows expanded domain of expression of *CUC2::CUC2-vYFP* unlike *plt3;plt5-2;plt7* (J',K'). White dotted circle marks upregulation of YFP expression near wounded area. Blue dotted line marks incision.

(L) Upregulation of *CUC2* transcript in injured wild type leaf at 12 h post injury as compared to control uninjured wild type leaves. Downregulation of *CUC2* transcript in injured *plt3;plt5-2;plt7* leaves as compared to control uninjured *plt3;plt5-2;plt7* leaves. (Welch's two-sample t-test; $^{**}P$ =0.002;$^{***}P$ =0.0004)

(M) Transcript level of *CUC2* upon induction of PLT5 with DEX treatment and with cycloheximide treatment.

Expression levels in (L) and (M) are normalized to *ACTIN2*. Error bar represents s.e.m. from three independent biological replicates

(N) ChIP-qPCR Analysis: ChIP-qPCR experiment in callus tissues shows direct binding of PLT5 fusion protein to the *CUC2* promoter. The results are shown as fold enrichment relative to *plt3;plt5-2;plt7* loss of function mutant. A strong binding of PLT5 is noticed at the fragment #1 (-1150 to -1448 bp) followed by a weak binding at #2 (-849 to -1149 bp) and no significant binding at the fragment #3 (-1 to -283 bp) of the upstream sequence of *CUC2*. Error bars show the standard error of the ChIP-qPCR reactions performed in triplicates.

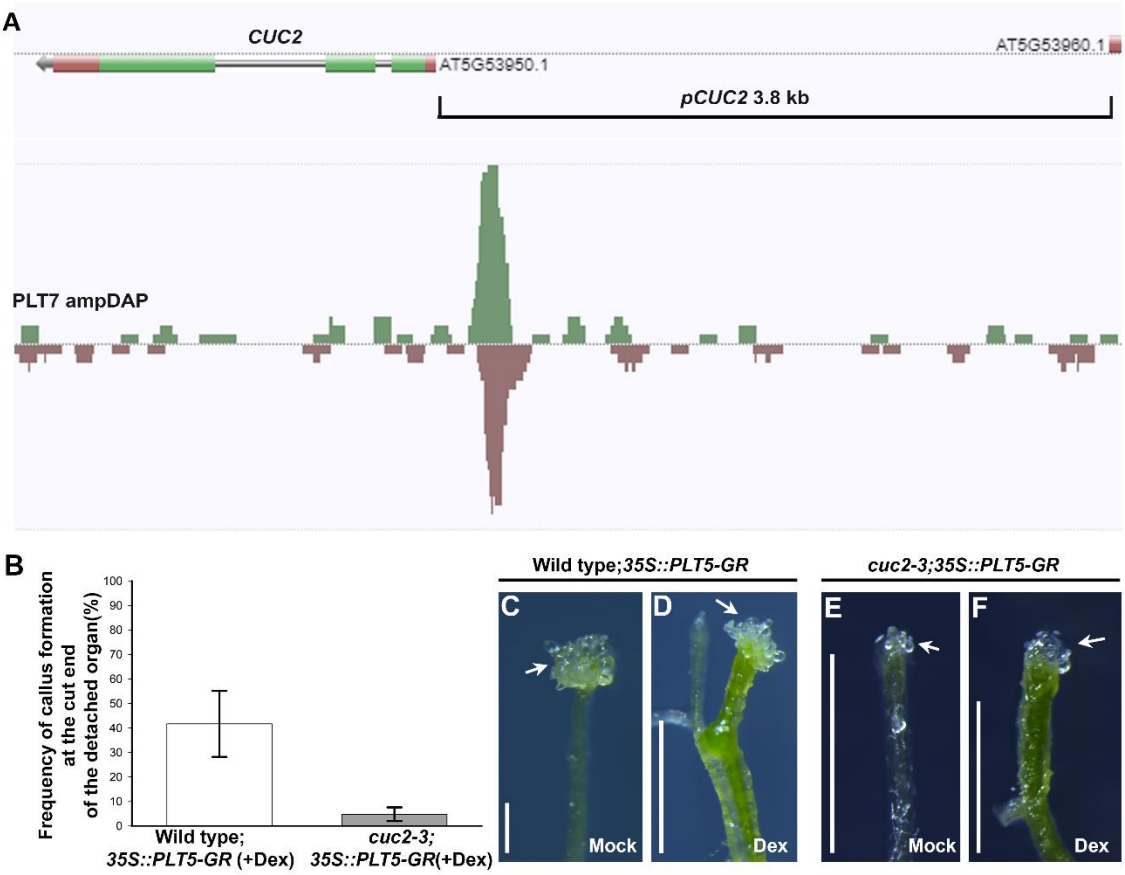

Figure S10: PLT acts through CUC2 during wound repair

(A) PLT7 binds the *CUC2* promoter (http://neomorph.salk.edu/). Indicated region shows *pCUC2*, which was used in the luciferase reporter assay.

(B) Frequency refers to the number of excised organs showing callus formation at the cut end. In addition to frequency, the extent of callus formation is lesser in *cuc2-3;35S::PLT5-GR*.

(C,D) Wild type;*35S::PLT5-GR* upon continuous DEX induction (n=12/15) (D) following excision shows increased extent of callus formation unlike in mock treated control (n=9/10) (C) at the detached end of root.

(E,F) *cuc2-3;35S::PLT5-GR* upon continuous DEX induction (n=15/20) (F) following excision shows no increase in extent of callus formation at the detached end of root as compared to mock treated control (n=16/20) (E).

Arrow: Callus formation. Scalebars:1 mm.

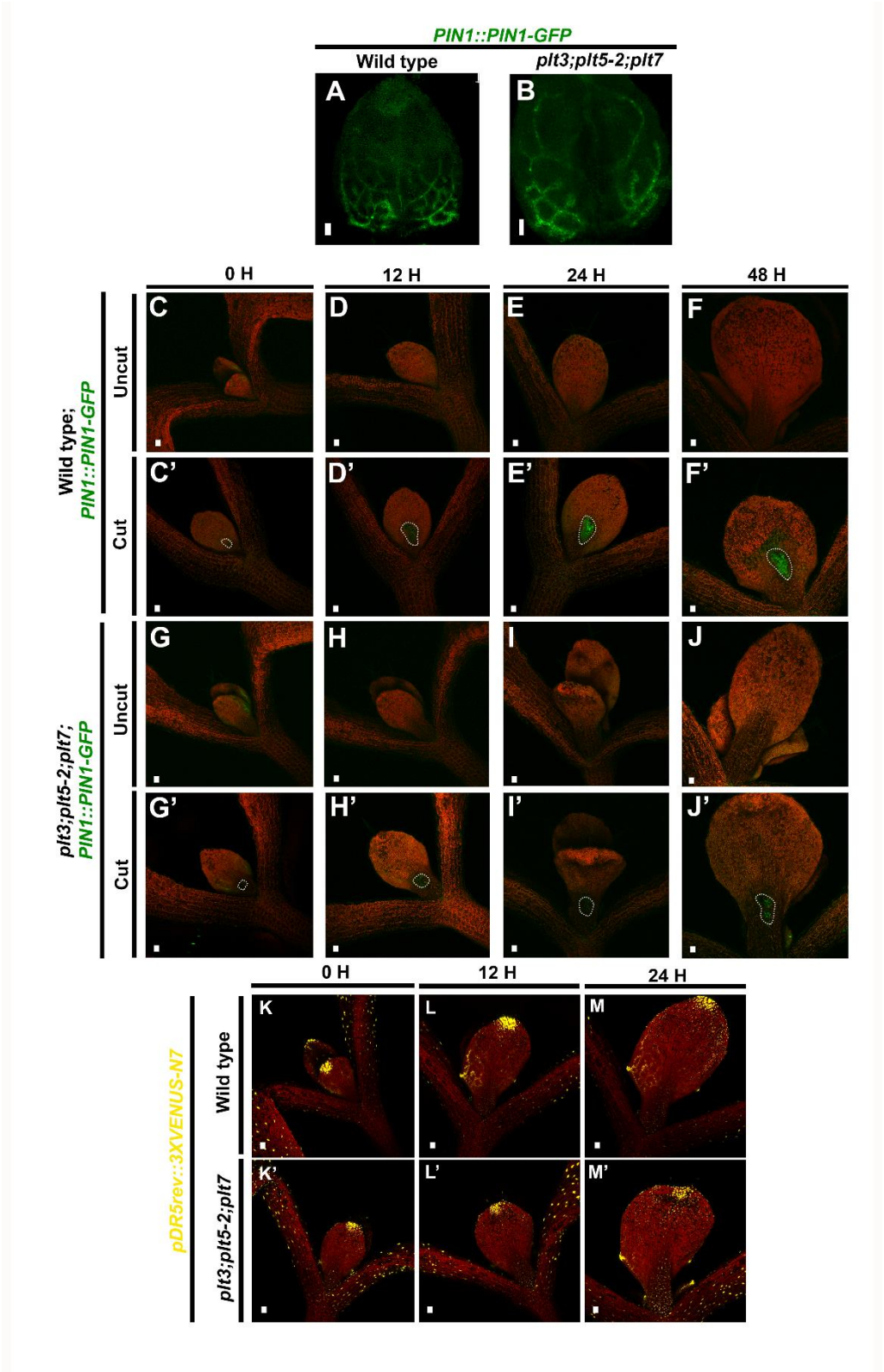

Figure S11: PIN1 expression and auxin response are not defective in *plt* mutant during normal development

(A,B) *PIN1::PIN1-GFP* expression in undamaged leaves of wild type (A) and *plt3;plt5-2;plt7* (B). PIN1 expression is visible in the basal part of the leaves in both wild type and *plt3;plt5-2;plt7*.

(C-J') Confocal time lapse images showing expression of *PIN1::PIN1-GFP* in wild type (C-F') and *plt3;plt5-2;plt7* (G-J'). (C-F) and (G-J) represent uninjured leaves while the remaining represent injured leaves in which injured areas are marked by white dotted lines.

(K-M') Confocal time lapse images showing expression of *pDR5rev::3XVENUS-N7* in wild type (K-M) and *plt3;plt5-2;plt7* (K'-M') uninjured leaves.

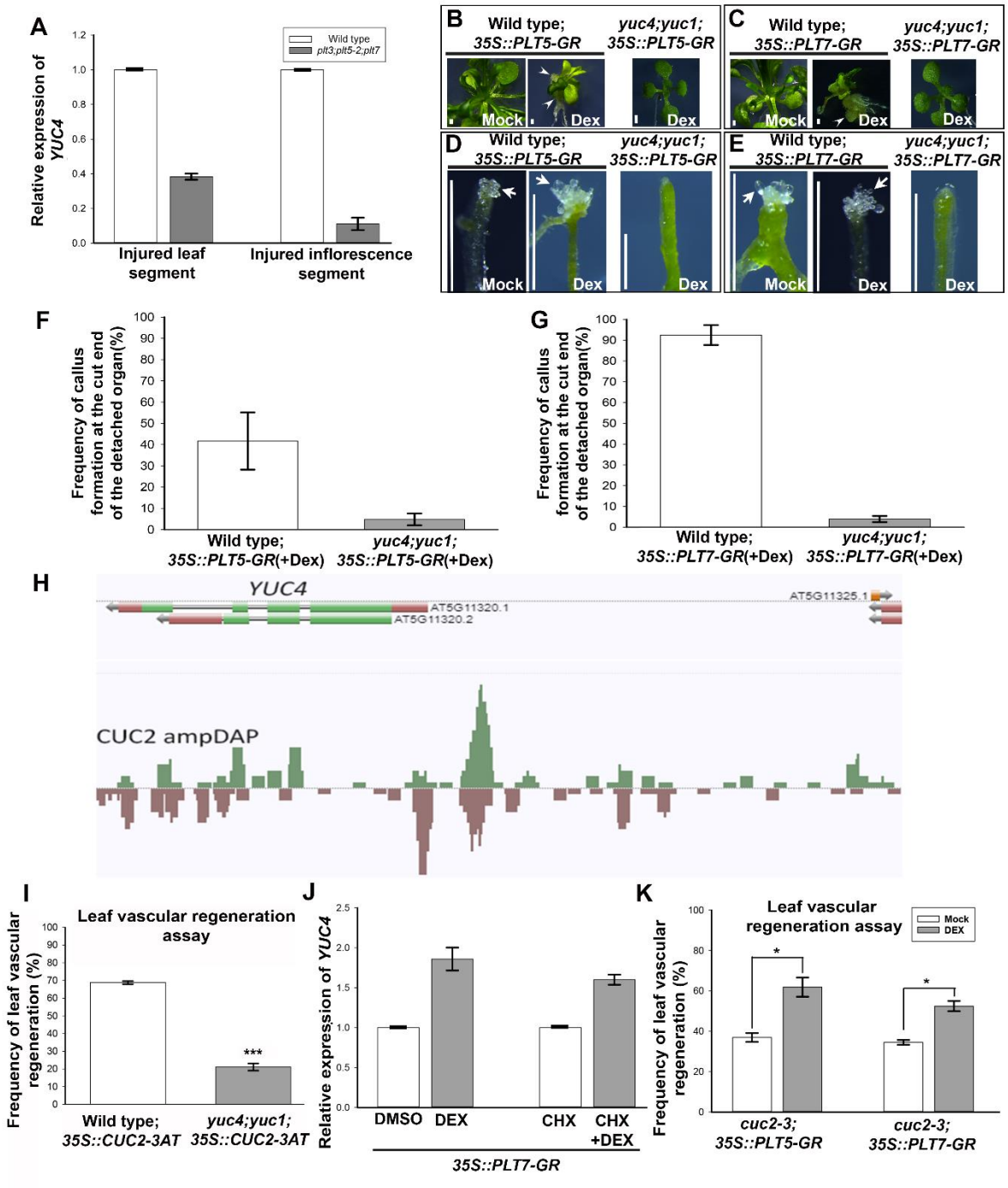

Figure S12: PLT acts though YUC4 during reprogramming and wound repair

(A) *YUC4* transcript level in injured and uninjured leaf and inflorescence stem segments of wild type and *plt3;plt5-2;plt7* mutant. Expression levels in A is normalized to *ACTIN2*. Error bar represents s.e.m. from three independent biological replicates.

(B) Growing seedlings of Wild type;*35S::PLT5-GR* upon DEX induction shows callus formation (arrowheads) from shoot and root leading to stunted growth of the plant, unlike mock treated control, which does not show any ectopic phenotypes. However *yuc4;yuc1;35S::PLT5-GR* does not show any cellular reprogramming even upon DEX induction.

(C) Growing seedlings of Wild type;*35S::PLT7-GR* upon DEX induction shows callus formation (arrowhead) from hypocotyl and root leading to stunted growth of the plant, unlike mock treated control, which does not show any ectopic phenotypes. However *yuc4;yuc1;35S::PLT7-GR* does not show any cellular reprogramming even upon DEX induction.

(D) Wild type;*35S::PLT5-GR* upon DEX induction (n=15/20) shows increased extent of callus formation unlike in mock treated control of detached organ (n=10/13). However *yuc4;yuc1;35S::PLT5-GR* (n=20/20) shows barely any callus formation upon DEX induction.

(E) Wild type;*35S::PLT7-GR* upon DEX induction (n=9/10) shows increased extent of callus formation unlike in mock treated control of detached organ (n=7/11). However *yuc4;yuc1;35S::PLT7-GR* (n=14/15) rarely shows callus formation upon DEX induction.

(F,G) Frequency refers to the number of excised organs showing callus formation at the cut end. In addition to frequency, the extent of callus formation at the wounded end of detached organ was extremely reduced in *yuc4;yuc1* as compared to wild type upon DEX induction of *35S::PLT5-GR* (F) and *35S::PLT7-GR* (G)

(H) CUC2 binds the *YUC4* promoter as shown by DAP-seq analysis (http://neomorph.salk.edu/).

(I) Frequency of leaf vascular regeneration in wild type;*35S::CUC2-3AT* and *yuc4;yuc1;35S::CUC2-3AT* (***P =2x10^{-6}).

(J) Transcript level of *YUC4* upon induction of *35S::PLT7-GR* with DEX treatment and with cycloheximide treatment at 4 h post injury. Expression levels are normalized to *ACTIN2*. Error bar represents s.e.m. from three independent biological replicates.

(K) Frequency of leaf vascular regeneration upon overexpression of *35S::PLT5-GR* and *35S::PLT7-GR* in *cuc2-3* mutant (Pearson's $\chi 2$ test).

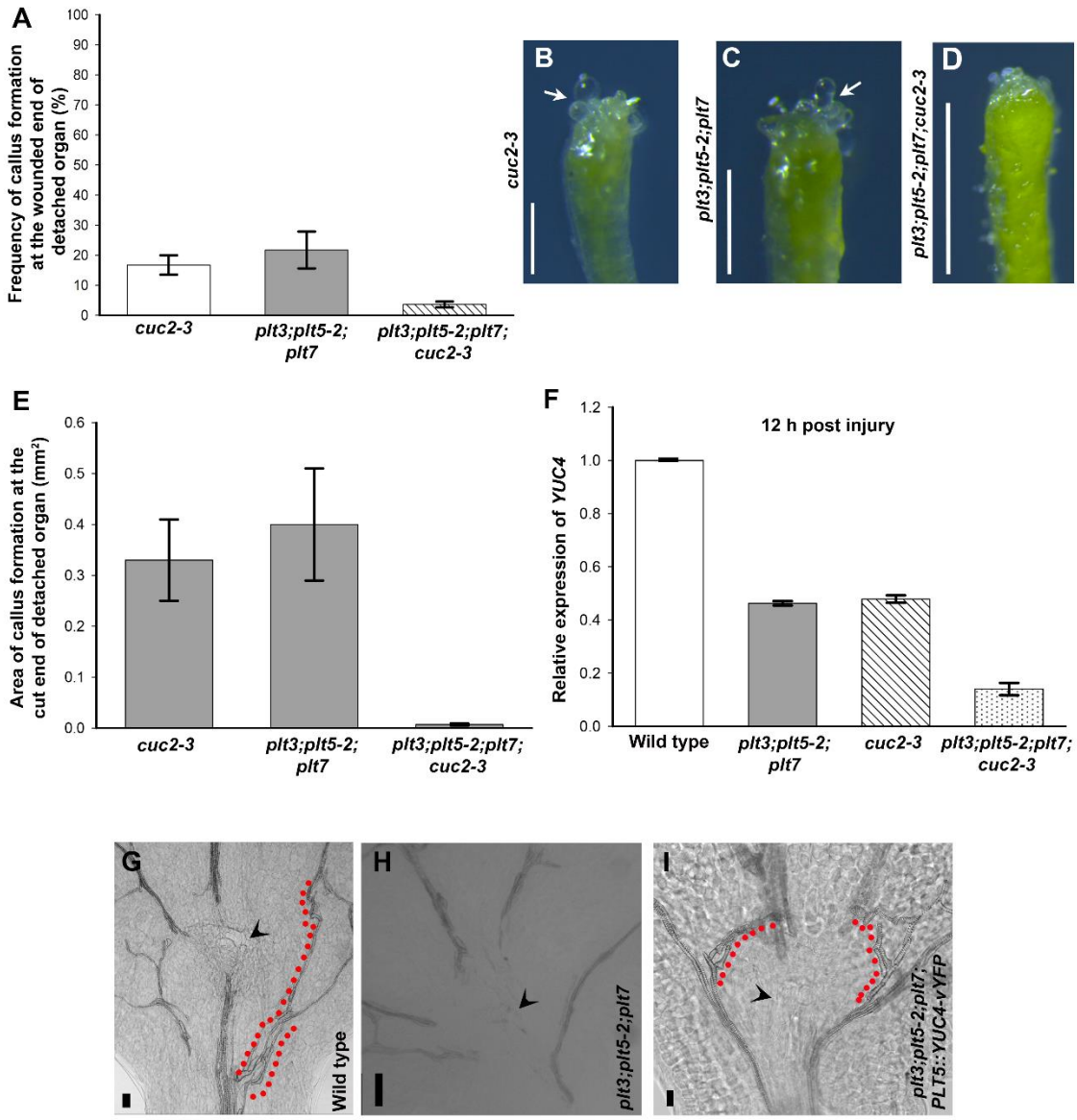

Figure S13: PLT and CUC2 regulate *YUC4* in a coherent feed forward loop

(A) Frequency refers to the number of excised organs showing callus formation at the cut end.

(B-D) In addition to frequency, extent of callus formation (white arrow) was drastically reduced in *plt3;plt5-2;plt7;cuc2-3* as compared to *cuc2-3* and *plt3;plt5-2;plt7* which showed moderate callus formation at the cut ends of detached organs.

(E) Area of callus formation at the cut end of detached organs of *cuc2-3;plt3;plt5-2;plt7* and *plt3;plt5-2;plt7;cuc2-3*.

(F) Relative expression levels of *YUC4* in wild type and mutants. Expression levels are normalized to *ACTIN2*. Error bar represents s.e.m. from three independent biological replicates.

(G-I) Vascular strand regeneration assay in wild type (G), *plt3;plt5-2;plt7* (H) and *plt3;plt5-2;plt7;PLT5::YUC4-vYFP* (I). Vascular strands fail to regenerate in *plt3;plt5-2;plt7* (H). Black arrowheads mark site of leaf incision. Red dotted lines mark regenerated vascular strands.

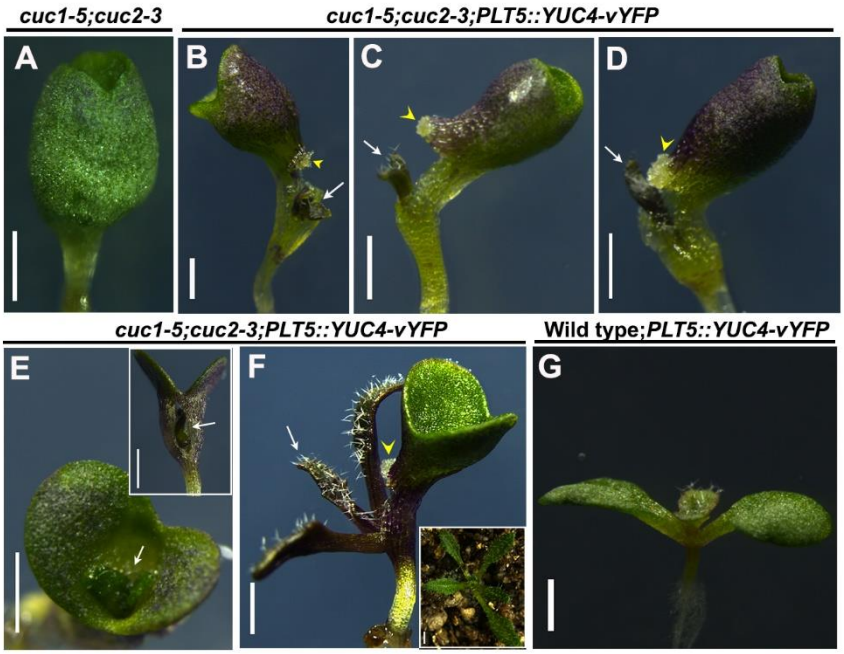

Figure S14: YUC4 rescued post embryonic development in *cuc1-5;cuc2-3* mutant

(A) Cup shaped cotyledon in *cuc1-5;cuc2-3* mutant (none out of 80 plants displaying cup shaped cotyledon produced shoot). (B-F) Reconstitution of local auxin biosynthesis gene *YUC4* in *PLT5* domain rescues post embryonic development, giving rise to fully developed leaves (marked by white arrows). Out of 48 plants with cup shaped cotyledon, 20 produced shoot from base of cotyledon. Callus formed at the base of cotyledon caused by the emergence of the shoot is marked by yellow arrowheads. (G) Wild type;*PLT5::YUC4-vYFP* showing normal shoot formation.

SUPPLEMENTARY INFORMATION

MATERIALS AND METHODS

Plasmid construction

To generate *PLT5::YUC4:vYFP* construct, 5.6kb upstream regulatory elements of *PLT5* and 1.93kb *YUC4* gene were separately amplified from genomic DNA and incorporated with *vYFP*. *plt3;plt5-2;plt7*, *cuc1-5(-/-);cuc2-3(+/-)* and *cuc2-1D* mutant plants were transformed using the construct. Similarly 1.7kb upstream regulatory element and 4.236kb *ATHB8* gene was incorporated with *vYFP* to generate the translational fusion construct *ATHB8::ATHB8-vYFP*. This construct was co-transformed with *PIN1::PIN1-GFP* into both wild type and *plt3;plt5-2;plt7* mutant to generate the double marker transgenic line. *OsPLT2 (LOC_Os06g44750.1)* was cloned under upstream regulatory elements of *Arabidopsis PLT5* gene and tagged with *vYFP*. This construct was transformed into *plt3;plt5-2;plt7*.

Decolourisation and tissue clearing for imaging vascular tissues

To visualize regenerating vascular strands, the injured leaf and inflorescence stem were carefully excised from the growing seedling 4 days post incision using Vannas straight scissors. Before proceeding for decolorization of chlorophyll, a longitudinal cut was made through the excised inflorescence stem using razor blade to expose the regenerating vascular strands. Both leaf and inflorescence stem were dehydrated and the chlorophyll was bleached by incubating the sample consecutively in 15%, 50%, 70% and 96% ethanol for 15 minutes each. Finally, the samples were incubated in absolute ethanol for 12 h. The sample was then rehydrated by transferring from 100% ethanol to 96%, 70%, 50% and finally 15% ethanol in the reverse order with 15 minutes incubation in each concentration of ethanol. Then the samples were incubated for 2-3 h in freshly prepared clearing solution consisting of 8 g chloral hydrate (Sigma-Aldrich), 1 ml 100% glycerol (Sigma-Aldrich) and 3 ml distilled water. The cleared samples were mounted on slides using the clearing solution with the abaxial surface of the leaf and the longitudinally cut surface of the inflorescence stem facing upward. Coverslip was placed carefully avoiding any bubble formation and curling of the tissues.

Sample preparation for qRT-PCR

Inflorescence stem abrasion was performed in wild type Columbia plants and *plt3;plt5-2;plt7* triple mutant. The injured part of inflorescence stem was harvested after four days and used for RNA extraction. Leaves were injured in the context of growing seedling and the entire seedling

without the root was taken for qRT-PCR. *PLT5*, *PLT7* and *CUC2* were induced using steroid inducible constructs in wild type;*35S*::*PLT5-GR*, wild type;*35S*::*PLT7-GR*, wild type;*35S*::*CUC2-GR* and *cuc1-5;cuc2-3;35S::PLT5-GR*. Prior to sample collection for RNA isolation, injured plants were transferred to MS plates containing 20 µM dexamethasone (DEX) or DMSO (Mock) (equal proportion as volume of DEX) followed by flooding the plate with liquid MS medium containing DEX or DMSO (Mock). In case of cycloheximide treatment, samples were pre-treated with 10 µM cycloheximide for 20 min (on MS medium with cycloheximide and flooded with liquid MS containing cycloheximide) followed by transfer to MS plates containing 20 µM DEX supplemented with 10 µM cycloheximide or to MS plates supplemented with DMSO and cycloheximide followed by flooding the plate with liquid MS medium of corresponding constituents. The wounded tissues were collected at 4 h or 8 h after treatment for RNA extraction.

ChIP-qPCR analysis.

600 mg fresh weight of five-day-old proliferating callus tissues derived from roots of *PLT5::PLT5-vYFP* and *plt3;plt5-2;plt7* were cross-linked in 1% formaldehyde (Sigma-Aldrich). The isolated chromatin was immunoprecipitated with anti-GFP antibody (5 µl per sample) (Clontech). After several washing steps, the protein–DNA cross-linking was reversed. Further, the DNA was cleaned using PCR Purification Kit (Qiagen).

REFERENCES FOR SUPPLEMENTARY INFORMATION

Bilsborough, G.D., Runions, A., Barkoulas, M., Jenkins, H.W., Hasson, A., Galinha, C., Laufs, P., Hay, A., Prusinkiewicz, P. and Tsiantis, M. (2011). Model for the regulation of Arabidopsis thaliana leaf margin development. *Proc. Natl. Acad. Sci. USA* **108**, 3424-3429. doi: 10.1073/PNAS.1015162108.

Kareem, A., Durgaprasad, K., Sugimoto, K., Du, Y., Pulianmackal, A.J., Trivedi, Z.B., Abhayadev, P.V., Pinon, V., Meyerowitz, E.M., Scheres, B. et al. (2015). PLETHORA genes control regeneration by a two-step mechanism.*Curr. Biol.* **25**, 1017-1030. doi: 10.1016/j.cub.2015.02.022.

Nikovics, K., Blein, T., Peaucelle, A., Ishida, T., Morin, H., Aida, M. and Laufs, P. (2006). The balance between the MIR164A and CUC2 genes controls leaf margin serration in Arabidopsis. *The Plant Cell*. **18**, 2929-2945. doi: 10.1105/TPC.106.045617.

Table S1: Synergistic interaction between PLT and CUC2 during vascular regeneration

Genotype	Frequency of leaf vascular regeneration (%)
plt3^{+}/-;*plt5-2*$^{+}$/-;*plt7*$^{+}$/-	70.52
cuc2-3^{+}/-	71.66
plt3^{+}/-;*plt5-2*$^{+}$/-;*plt7*$^{+}$/-;*cuc2-3*$^{+}$/-	36.80

Table S2. Oligonucleotide primers used for cloning and qRT PCR (5'-3')

Primer name	Forward primer	Reverse primer
qRT-PLT5	CTACTCCGGTGGACACTCGT	CGTTCTTCTTCGGAGTAGGC
qRT-PLT7	TTTCCTCGGTGATTCCTTTG	TGACGTGGATCGTAGAATGG
qRT-YUC4	TCCATAATATTAGCGACTGGGTA	CCCTTCTCTCCTTTCCATCC
pCUC2 LUCR	GGGGACAAGTTTGTACAAAAAAG CAGGCTttaattctacattttgtttgg	GGGGACCACTTTGTACAAGAA AGCTGGGTtgttttgaagaagaagataaa
ATHB8 promoter	GGGGACAACTTTGTATAGAAAAG TTGTTCGGATAAACCAATTTTCAA ATG	GGGGACTGCTTTTTTGTACAAA CTTGTCTTTGATCCTCTCCGAT CT
ATHB8 gene	GGGGACAAGTTTGTACAAAAAAG CAGGCTGTATGGGAGGAGGAAGC AATAATAGTCA	GGGGACCACTTTGTACAAGAA AGCTGGGTTTATAAAAGACCA GTTGAGGAACATGAAGC

Additional primers used in this study have been previously described (Kareem *et al*. 2015)

Table S3. Primers used for ChIP-qPCR

Primer name	Forward primer	Reverse primer
CUC2-ChIP #1	ACATTTTTGGGTGGGAAAT	AGAGAAGATATTTATGCTGCCT
CUC2-ChIP #2	GATTTGCAACCTGTAACTTC	TGTCAGCACAGTACATGATT
CUC2-ChIP #3	TCTTCTCTACGACTTTCTGG	TAAGAAGAAAGATCTAAAGCTTTT G
ACT7-ChIP	CGTTTCGCTTTCCTTAGTGTT AGCT	AGCGAACGGATCTAGAGACTCAC CTTG